THE UNIVERSITY OF MICHIGAN
COLLEGE OF ENGINEERING
Department of Electrical Engineering
Space Physics Research Laboratory and Electronic Defense Group

Final Report

Period Covering October 3, 1958, to November 30, 1959

A TWO-FREQUENCY BEACON FOR HIGH-ALTITUDE IONOSPHERE ROCKET RESEARCH

L. W. Orr P. G. Cath B. R. Darnall

UMRI Project 2816-3

under contract with:

DEPARTMENT OF THE ARMY
BALLISTIC RESEARCH LABORATORY
PROJECT NO. DA-5B03-06-011-ORD (TB 3-0538)
CONTRACT NO. DA-20-018-509-ORD-103
ABERDEEN PROVING GROUND, MARYLAND

administered by:

THE UNIVERSITY OF MICHIGAN RESEARCH INSTITUTE ANN ARBOR

December 1959

TABLE OF CONTENTS

LIST OF ILLUSTRATIONS

ABSTRACT

The design of a two-frequency beacon is described. The fully transistorized beacon transmits at frequencies of 37 and 148 megacycles, with powers of 100 and 20 milliwatt respectively. Loop antennas are used at both frequencies and telemetry is provided on the 148 Mc signal for measuring the nose-cone temperature.

The crystal oscillator is temperature stabilized by the heat of fusion method and has a frequency stability of better than one part in 10^8 during flight.

Also discussed are the transmitter powers required at the two frequencies and thermal design considerations of the beacon.

A short summary is given of the results of the firing on November 10, 1959.

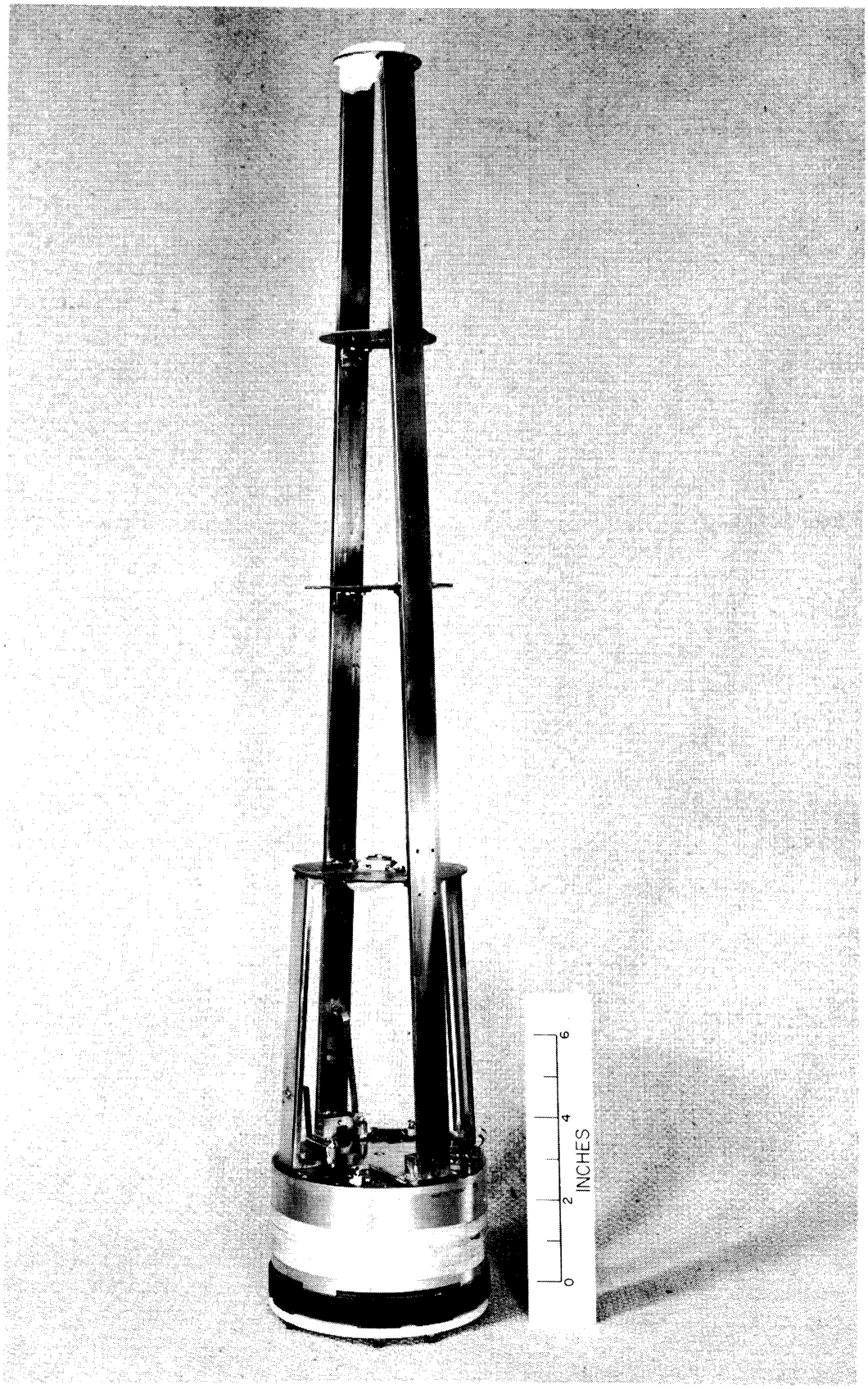

Fig. 1 Beacon With Antenna Completely Assembled

1. INTRODUCTION

A vertical profile of electron density in the ionosphere was measured by the two-frequency method to a height of roughly 1100 miles on 10 November 1959. This required a five-stage rocket vehicle, a two-frequency beacon transmitter in the nose of the fifth stage, and a ground station for receiving the beacon signals. The ground station was furnished and staffed by the Ballistic Research Laboratory, Aberdeen Proving Ground, Maryland. The rocket vehicle and beacon transmitter were developed and operated by The University of Michigan under contract with the Ballistic Research Laboratory. The development and operation of the beacon is the subject of this report.

Figure 1 shows the complete two-frequency beacon package, together with its antenna system. Because weight in the nose was needed for flight stability, no particular attention was given to lightening the payload and, in fact, an antenna 1000 grams heavier than the one first designed was required. As seen in the figure, the beacon package weighs 1800 grams while the antenna assembly (heavy model) weighs 1760 grams.

The primary purposes of this five-stage rocket experiment were:

a. Measurement of the electron density profile to a height of roughly 1000 miles.
b. Proving in the vehicle.

Secondary purposes of the experiment were:

a. Examination of the frequency stability achievable in the rocket environment.
b. Measurement of nose cone-temperature.
c. Measurement of the package temperature.

The minimum requirements specified by the Ballistic Research Laboratory for the two-frequency beacon are as follows:

1. A 100-milliwatt transmitter at 37 Mc.
2. A 20-milliwatt transmitter at exactly 4 times the first frequency and phase locked to it.
3. A frequency stability* of one part in 10^6.

*A single frequency probe was contemplated at the beginning of the project with a frequency stability requirement of better than one part in 10^7. Since the method had been developed to satisfy this, it was decided to continue with the high stability beacon design. The frequency stability actually achieved in the flying models was one part in 10^8 or better.

A highly successful firing took place at 0700 hours from Wallops Island, Virginia, on 10 November 1959. Signals were received continuously on both frequencies for 1500 seconds of flight at the Wallops ground station, and for 1515 seconds at the Aberdeen Proving Ground station. The telemeter record obtained at Wallops Island gave measurements of the nose cone temperature and gave one point in the temperature rise of the package during flight (Section 6).

2. REQUIRED TRANSMITTER POWER

The transmitter power required for the two-frequency nose-cone beacon depends on a number of factors including space attenuation, cosmic noise, antenna gains and efficiency, effective bandwidth of the ground receiver, and minimum signal-to-noise ratio required for phase lock of the tracking filter. A review of the various factors is presented here, and the margin of safety (gain margin) is calculated for the nominal values of power chosen for the beacon.

For free space propagation, the power received from the rocket-borne transmitter is given by

$$P_r = \frac{P_t G_t A_r}{4\pi D^2} = \frac{P_t G_t G_r c^2}{(4\pi DF)^2} \qquad (1)$$

where:

P_t is the transmitted power,

G_t and G_r are the antenna power gains,

A_r is the effective area of the receiver antenna

$$A_r = G_r \lambda^2/4\pi = G_r c^2/4\pi F^2$$

D is the transmission path length,

F and λ are the frequency and wavelength of the transmission, and

c is the velocity of light.

A convenient formula for the space attenuation in decibels when using dipole antennas ($G_t = G_r = 1.6$ power gain) can be derived from (1):

$$\text{Space atten.} = 32.6 + 20\ (\log D + \log F)\ \text{decibels}\ , \qquad (2)$$

where D and F are expressed in <u>miles</u> and <u>megacycles</u>.

2.1. POWER REQUIRED AT 37 MC FOR D = 1000 MILES

At this frequency the cosmic noise level is so high that the noise figure of the receiver need not be considered. Because of the small size of the nose

From: Victor W. Richard, Operation And Application
Of The Ballistic Research Laboratories' Tracking Filter.
13th Annual Conference Of The Instrument Society of America; Sept. 1958

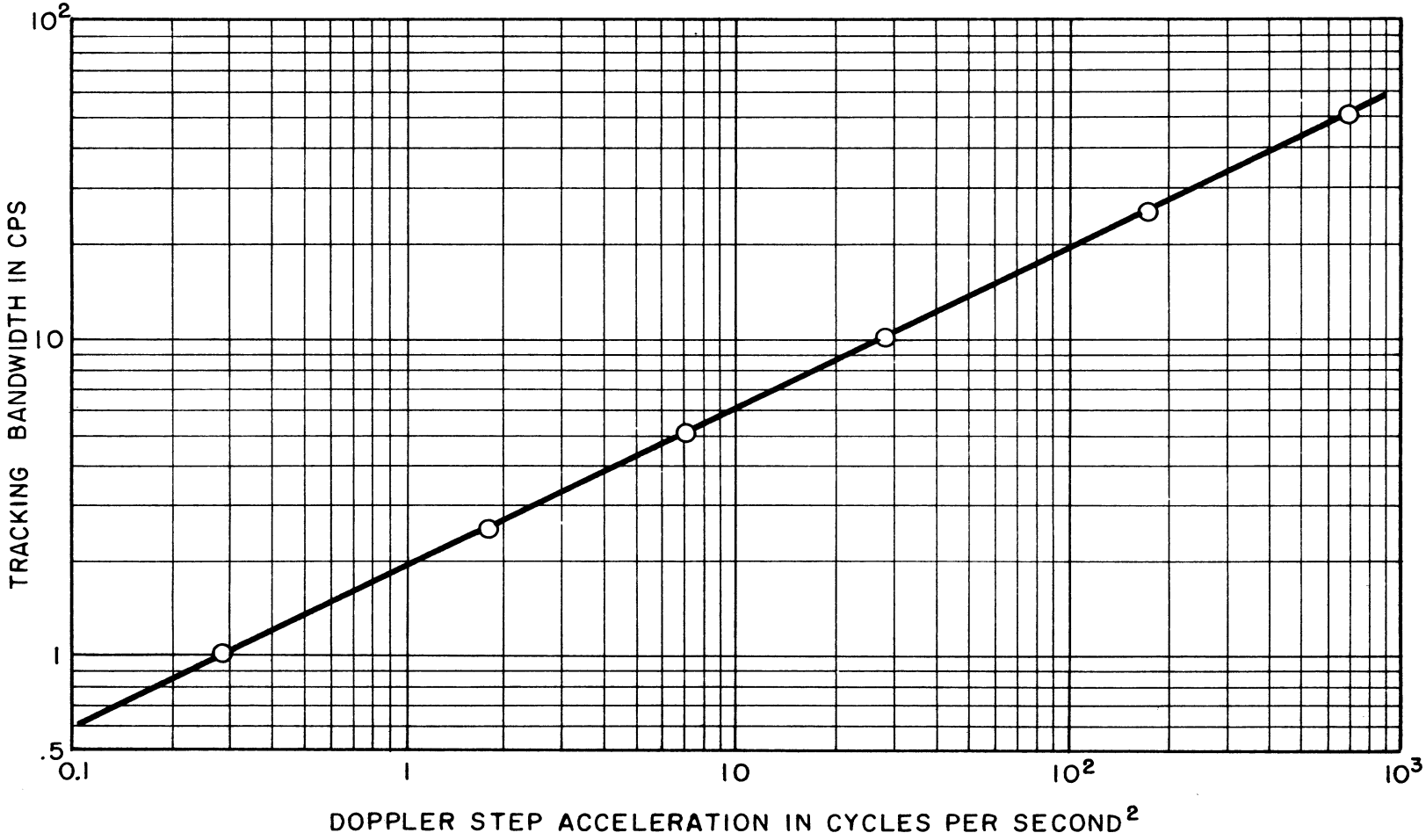

Fig. 2 Tracking Bandwidth vs. Doppler Step Acceleration

cone, a full-size loop antenna cannot be used, and the inefficiency of the 37 Mc antenna must be considered. The receiving system in the ground station contains a tracking filter which tracks with marginal locking with a phase jitter of 30° rms, and this requires a signal-to-noise ratio of 6 db.

The Doppler acceleration in cycles per sec^2 is given by the expression

$$\dot{D} = \frac{FA_g}{30.6} \qquad (3)$$

where F is the frequency of the radio wave in megacycles per second and A_g is the radial acceleration in g's. This expression gives the maximum Doppler acceleration* at 80 g's for the 37 megacycle transmission as 96.7 cycles per sec^2.

The required tracking filter bandwidth is obtained from Fig. 2. A Doppler acceleration of 96.7 cycles per sec^2 requires a bandwidth of 19 cps. The next larger bandwidth has to be used for the filter which is B = 25 cps.

The space attenuation is first found from Eq. (2)

Space atten. = 32.6 + 20 (log 1000 + log 37)	= 124.0 db
Loss due to antenna inefficiency	= 16 db
Total signal attenuation	= 140.0 db

Mean cosmic noise temperature** at 37 Mc	= $T_n = 2 \times 10^4$ °K
Minimum tracking filter bandwidth	= B = 25 cps
Boltzmann's constant	= $k = 1.38 \times 10^{-23}$ joules/°K
Equivalent input noise power to receiver	= $kT_nB = 6.9 \times 10^{-18}$ watt
Signal power required for marginal locking of tracking filter (6 db above noise)	= $4kT_nB = 2.8 \times 10^{-17}$ watt

Transmitter power required is 140 db above 2.8×10^{-17} watt or

$$P_t = 2.8 \times 10^{-3} \text{ watt} \quad . \qquad (4)$$

A nominal power of 100 milliwatts was suggested for the 37-Mc output. This gives a gain margin of 15 db. If the gain of the helical receiving antenna is now considered (approximately 8 db above dipole), a gain margin of 23 db is obtained.

2.2. POWER REQUIRED AT 148 MC FOR D = 1000 MILES

At this frequency the cosmic background noise is much lower, and contribu-

*The largest step in acceleration occurs at stage 4 burnout, and this does not exceed 80 g's.

**F. T. Haddock, private communication.

tions due to internal receiver noise must be considered. A noise figure F = 2 (or 3 db) will be assumed.

Equation (3) gives a value of 387 cycles per sec^2 for the maximum Doppler acceleration. Using Fig. 2 we find that a tracking filter bandwidth of 50 cps is needed, this being the next larger bandwidth above 38 cps.

Space atten. [Eq. (2)] = 32.6 + 20 (log 1000 + log 148)	= 136 db
Loss due to inefficiency of rocket-borne high-frequency loop antenna	= 3 db
Total	139 db

Minimum tracking filter bandwidty at 148 Mc, B = 50 cps
Receiver reference temperature T_r = 300°K
Equivalent noise power at receiver input due to internal receiver noise = $(F-1)kT_rB$ = 300kB
Mean cosmic noise temperature* at 148 Mc, $T_n \cong$ 700°K
Cosmic noise power = kT_nB = 700kB
Equivalent receiver input noise power = 1000kB = 6.9×10^{-19} watt
Signal power for 30° jitter (S/N = 6 db) = 2.8×10^{-18} watt
Transmitter power required 139 db above 2.8×10^{-18} watt or

$$P_t = 2.2 \times 10^{-4} \text{ watt} \qquad (5)$$

A nominal transmitter power of 20 milliwatts was suggested for the high-frequency unit. This would give a gain margin of approximately 19 db. Allowing for the added gain of the ground receiving antenna, the gain margin increases to at least 27 db.

*F. T. Haddock, private communication

3. NOSE-CONE ANTENNA DESIGN

Physically the nose-cone antennas for both frequencies are trapezoidal loops, constructed of brass with fiberglass spacers. The complete antenna mounted on the beacon package is shown in Fig. 1. The antenna loops are mutually perpendicular. With this arrangement it is found that the radiation pattern of either is essentially unaffected by the presence of the other.

The dimensions of the 37 Mc antenna are governed by the inside dimensions of the nose cone and are shown in Fig. 3. Round fiberglass spacers are inserted at heights of 7, 14, and 20 inches and are held in place by brass brackets. The legs of the 37 Mc antenna loop are constructed from 3/16 in. solid brass rather than the lighter 1/32 in. channel, to obtain a proper overall center of gravity for the complete final stage of the missile.

The maximum allowable dimensions of the 148 Mc antenna are determined primarily by the shape of the resultant radiation pattern. It turns out that a multilobed radiation pattern results if the circumference of the antenna loop exceeds 0.3 wavelengths* . Another size limitation arises from the fact that the size of the tuning capacitor decreases to a point of impracticability as the loop is enlarged. Final dimensions for the 148 Mc antenna are shown in Fig. 3.

Radiation patterns were obtained through the cooperation of the research staff at Ballistic Research Laboratories. The departure from a circular radiation pattern was less than one db for the 37 Mc antenna, and less than 3 db for the 148 Mc antenna, when plotted in the plane of either antenna.

Electrical features of the antennas include current feed loops and temperature compensation in the tuning capacitors.

Current feed loops (Fig. 4b) are used in preference to voltage feed (Fig. 4a) for three reasons; (a) it simplifies the construction and eliminates extra components and transmission cables; (b) current feed loops were found experimentally to be as efficient as the voltage feed; (c) impedance matching is simpler and is independent of tuning in a current-fed antenna. The loop sizes are adjusted so that the antenna input impedance becomes $50 + j0\ \Omega$ at resonance, which is the proper load impedance for the transmitters. Final current feed loop dimensions are illustrated in Figs. 5 and 6. A Hewlett Packard VHF Signal Generator (608-D), Bridge (803-A), and Detector (417-A) were used to measure the antenna impedances as functions of frequency. The results of these measure-

*Mr. Victor W. Richard, private communication.

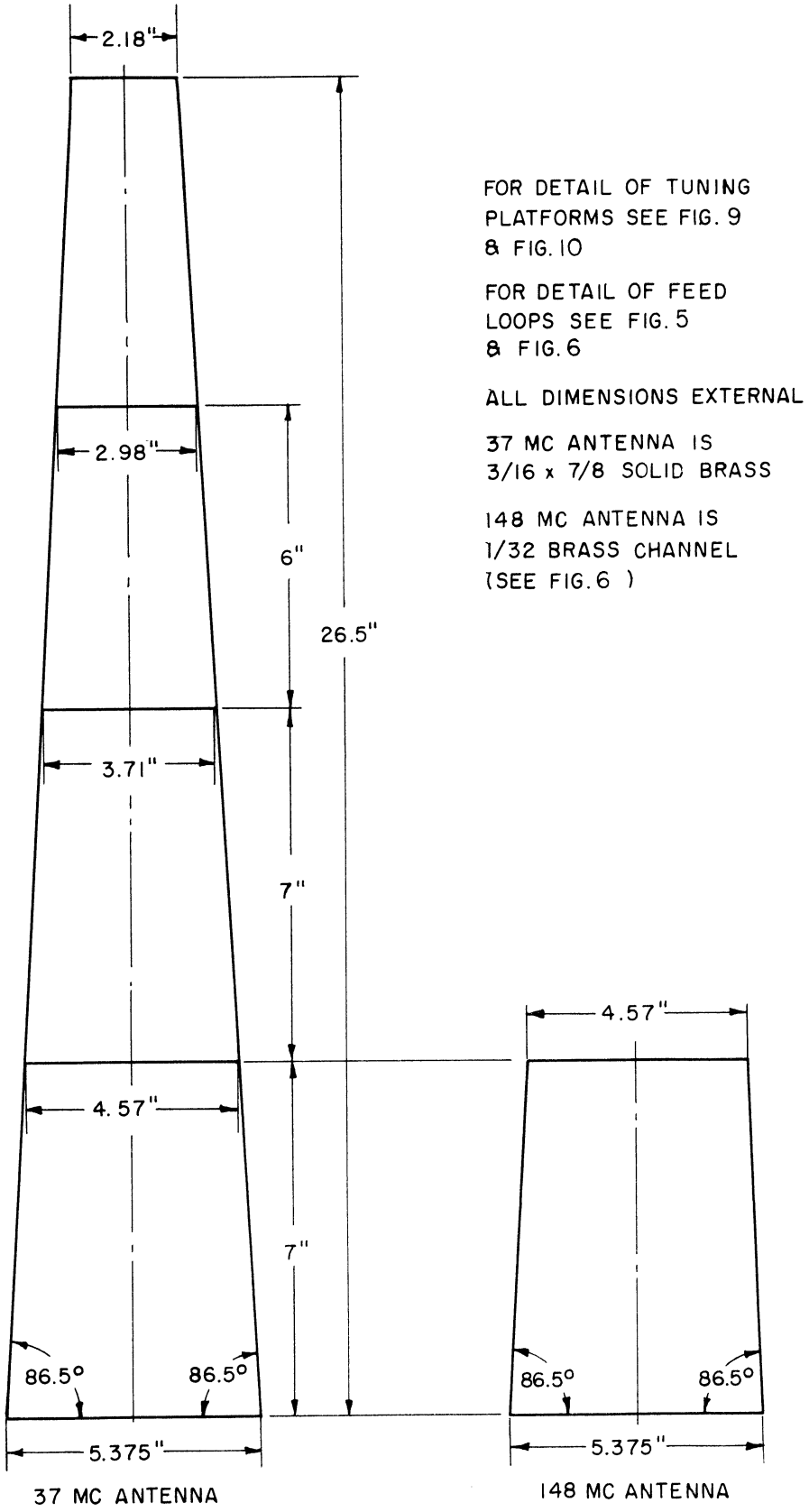

Fig. 3 Antenna Dimensions

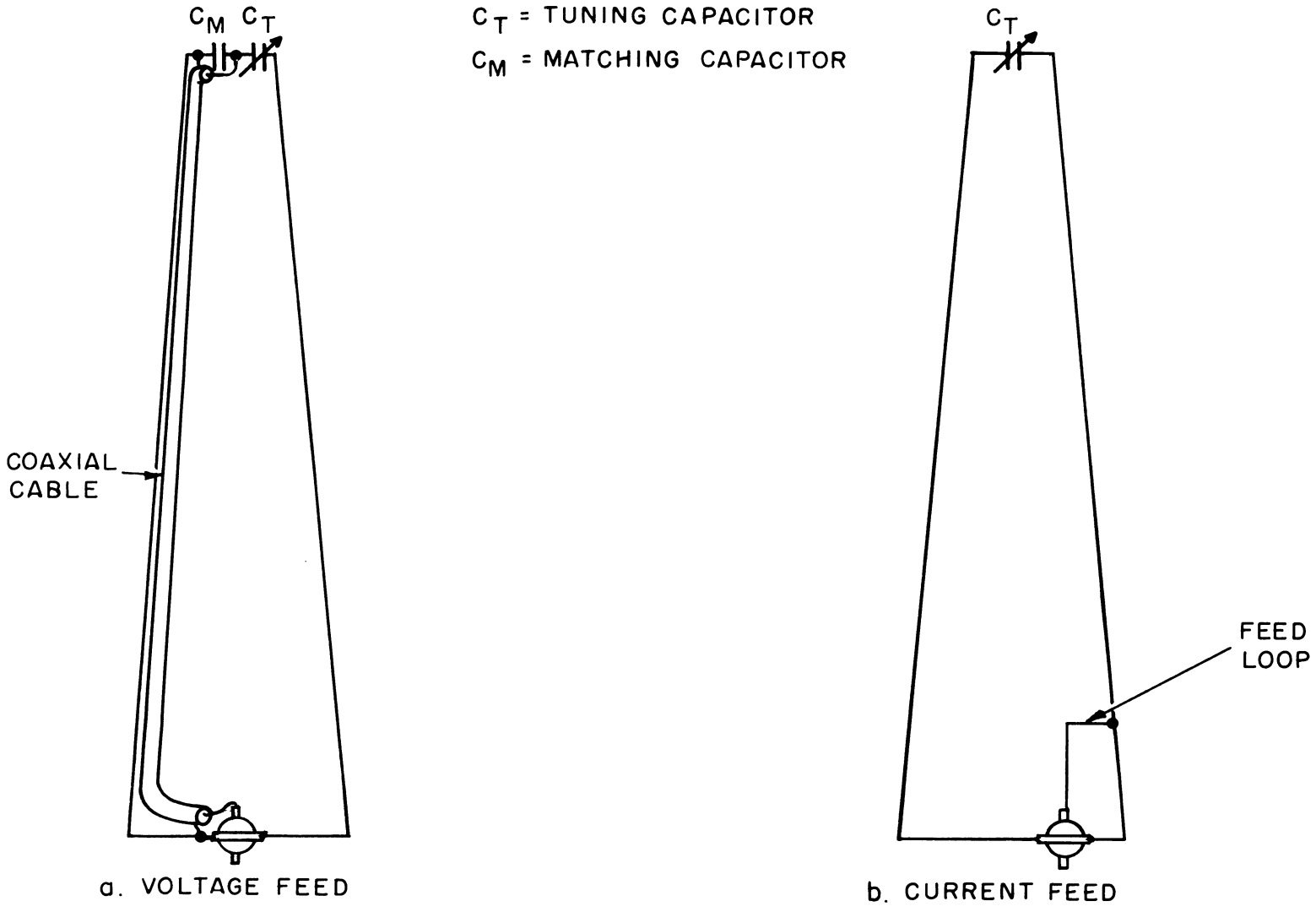

Fig. 4 Antenna Feed Methods

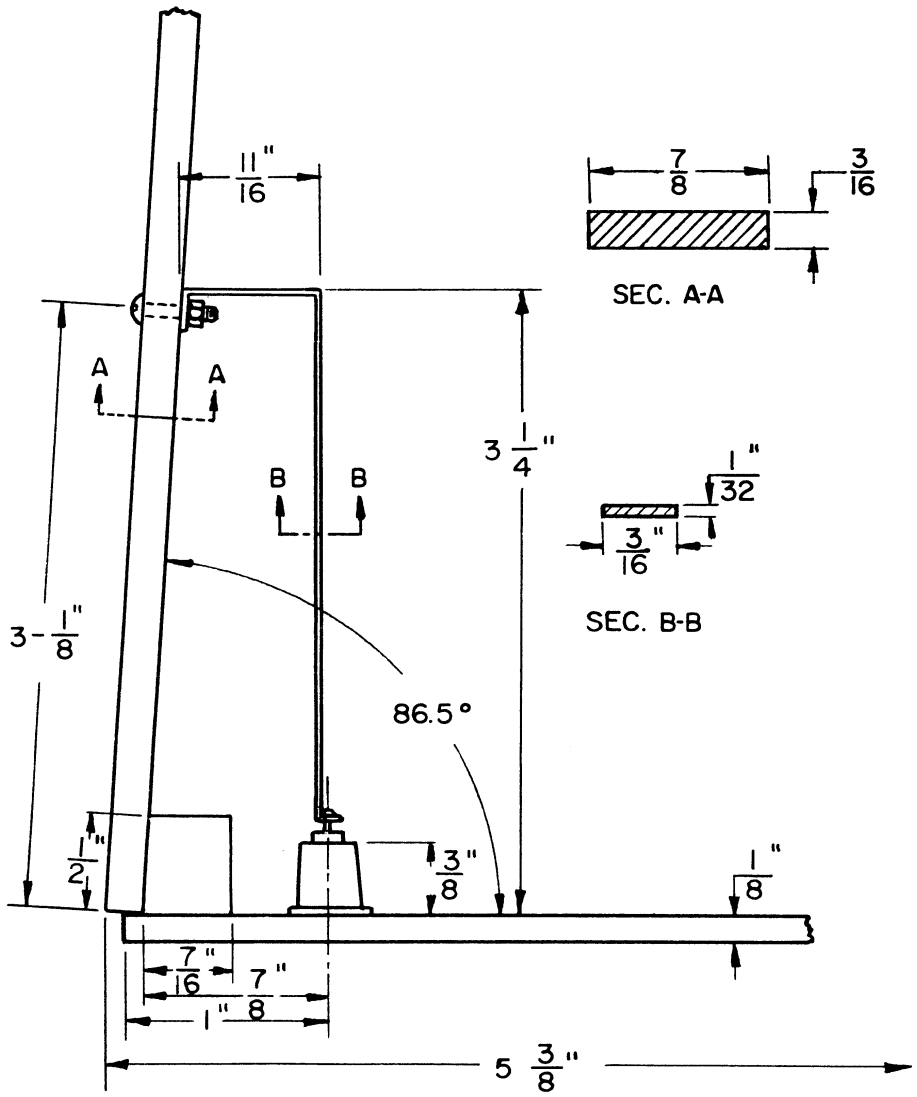

Fig. 5 Feed Loop 37 MC Antenna

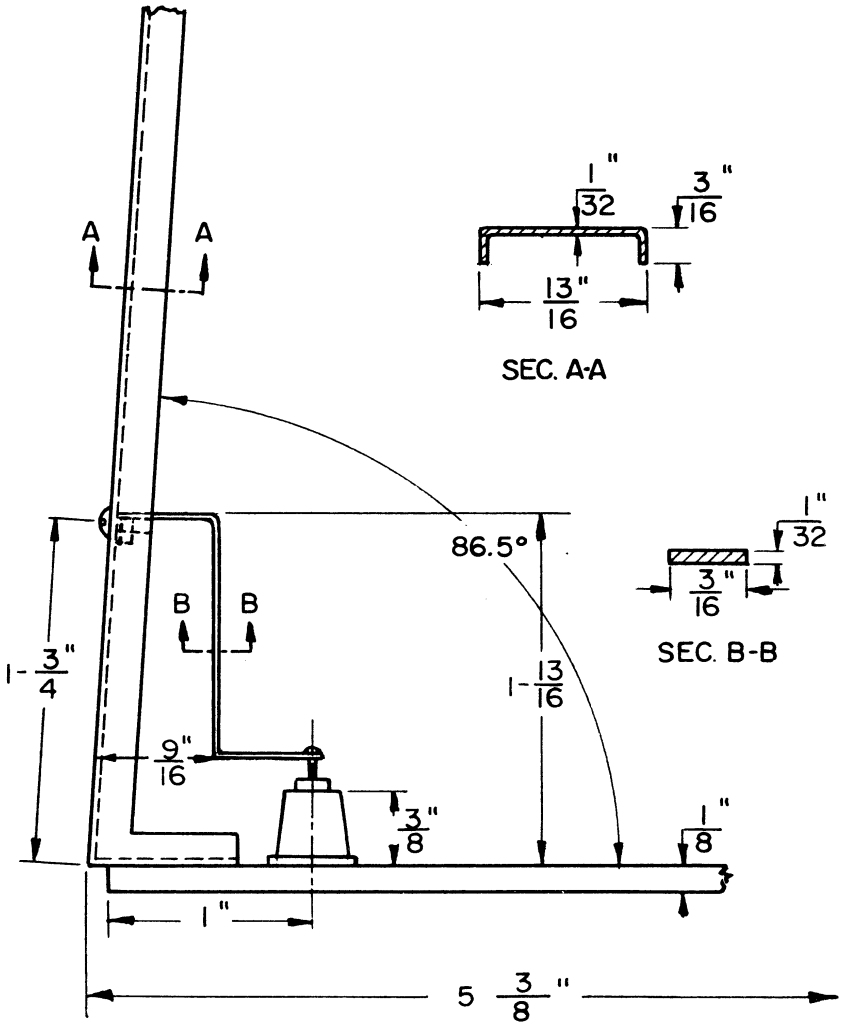

Fig. 6 Feed Loop 148 MC Antenna

ments are shown in Figs. 7 and 8. These, by the way, are the impedances measured at the input of the transmission line connecting the antenna to the bridge. The antenna input impedance at the feed point, when plotted on the Z-θ chart, will approximate a circle with the points 0 and 50 Ω lying on a diameter.

Tuning of each antenna is accomplished by means of a ceramic trimmer with associated padding capacitors determined by operating frequency and desired tuning range. The capacitor values were determined with the antenna placed inside the nose cone. The nose cone lowers the resonant frequency of the 37 Mc antenna by about 300 kilocycles. Figures 9 and 10 illustrate the arrangement of components on each tuning platform and a diagram of the circuit used. To facilitate tuning of the 148 Mc antenna while enclosed by the nose cone, the 37 Mc tuning capacitor (C-2 in Fig. 9) is offset to allow insertion of a tuning wand to the trimmer of the 148 Mc antenna.

Additional care was necessary in choosing capacitors to insure adequate frequency stability of the antennas over the anticipated range of flight temperatures. To determine the correct temperature compensation a heat run was made using the experimental set-up shown in Fig. 11.

The experiment determines first the resonant frequency of the 37 Mc antenna as a function of temperature. The resonant frequency is the frequency at which the antenna input impedance has an imaginary part equal to zero. In our case the input impedance at resonance is 50 + j0 Ω, providing the ideal match to the 37 Mc transmitter.

Secondly the variation in phase angle was measured for the 37 Mc antenna as a function of temperature. This is the phase angle of the antenna input impedance at a fixed frequency. It is a measure of the mismatch between the antenna and the transmitter, that occurs due to temperature changes. The results of both these experiments, performed on a temperature compensated antenna, are plotted in Fig. 12.

The change in phase angle of the 37 Mc antenna impedance is a direct result of the high Q of this antenna structure. The Q was measured to be 160. A combination of capacitors with different temperature coefficients (Fig. 9) was chosen to minimize both the variation in phase angle and in resonant frequency.

The 148 Mc antenna did not require special compensation since its phase angle at constant frequency input, did not vary noticeably in any of the temperature runs.

Final antenna characteristics were as follows:

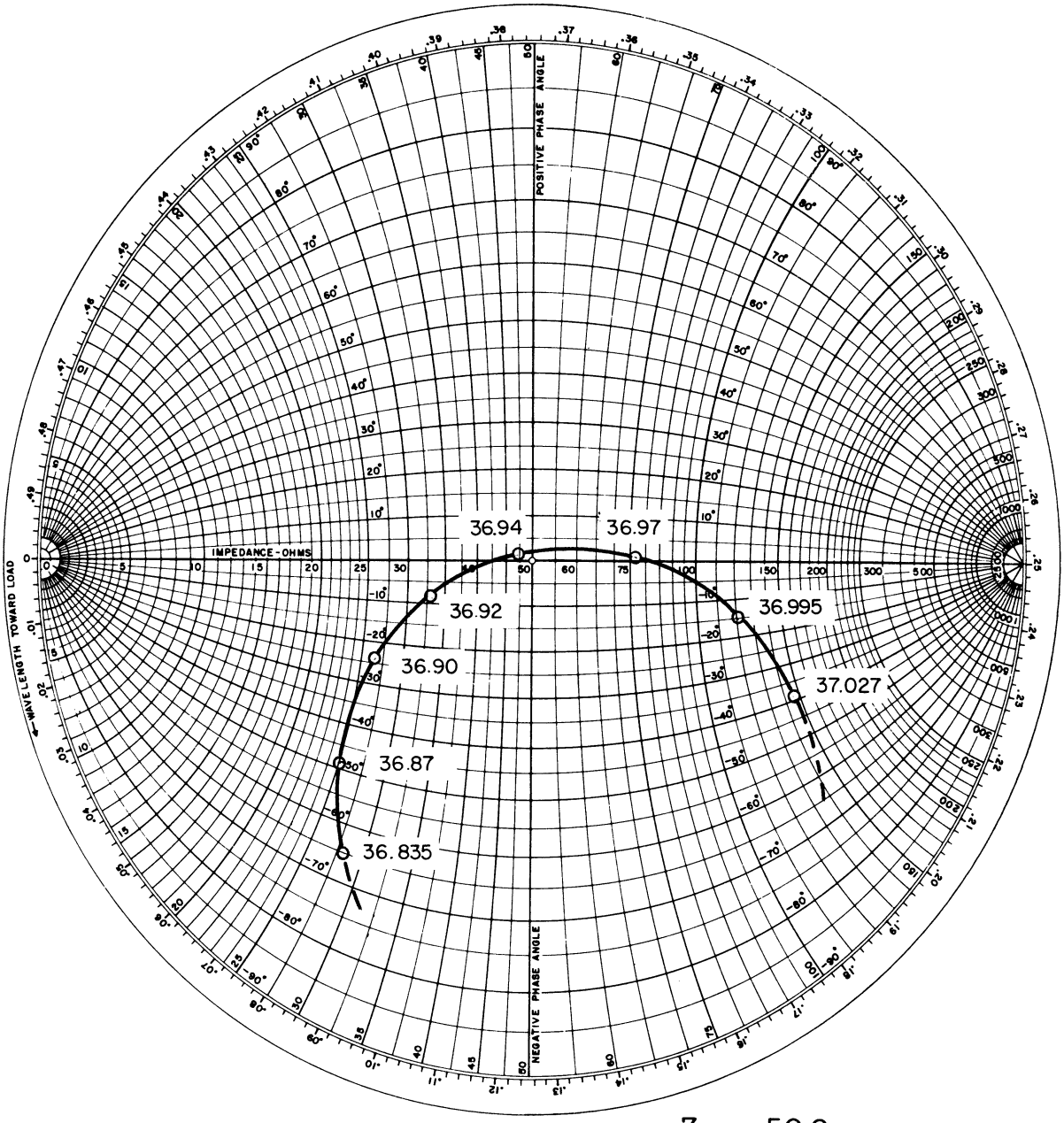

Fig. 7 Impedance vs. Frequency 37 MC Antenna

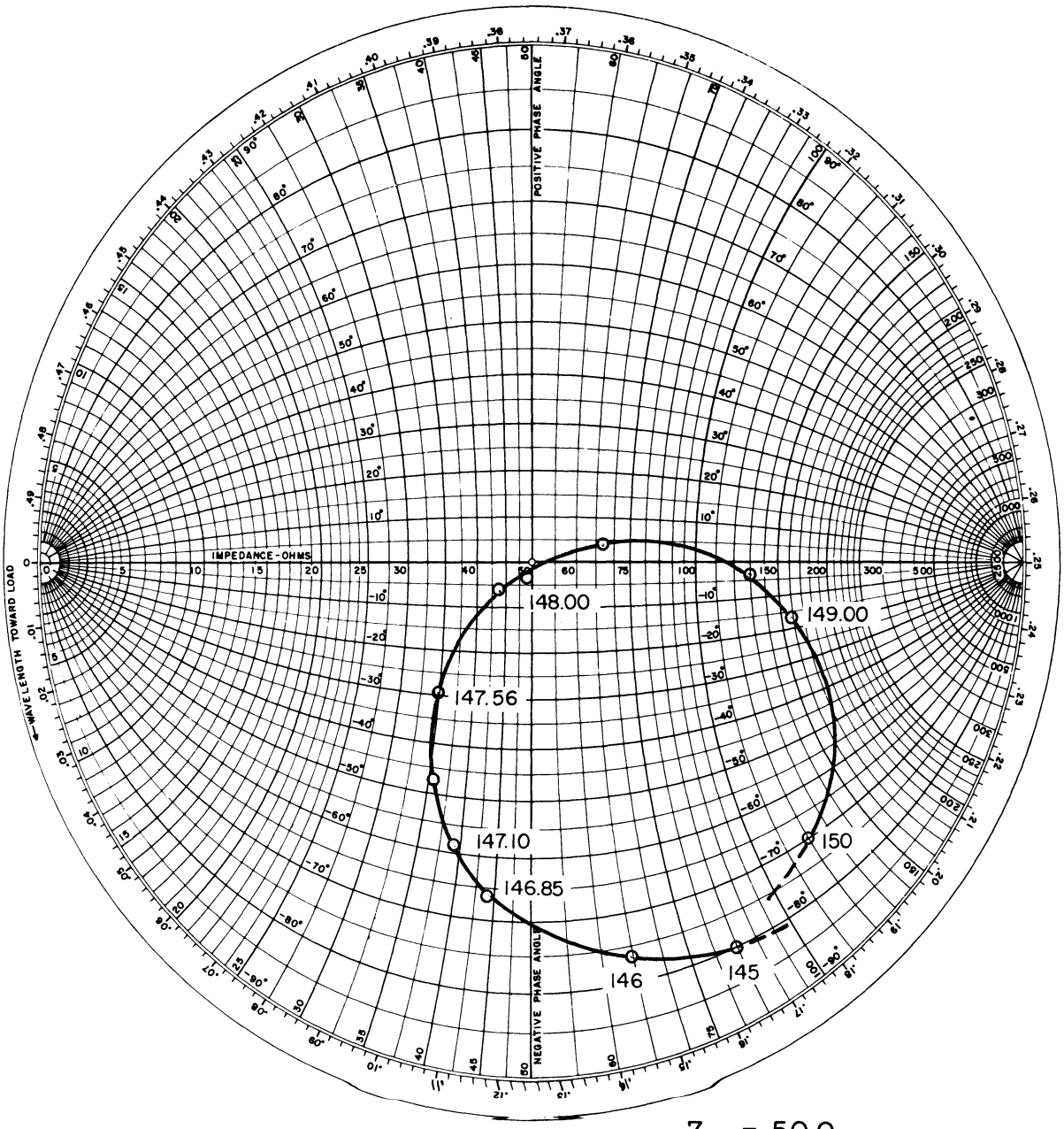

Z - θ CHART

Fig. 8 Impedance vs. Frequency 148 MC Antenna

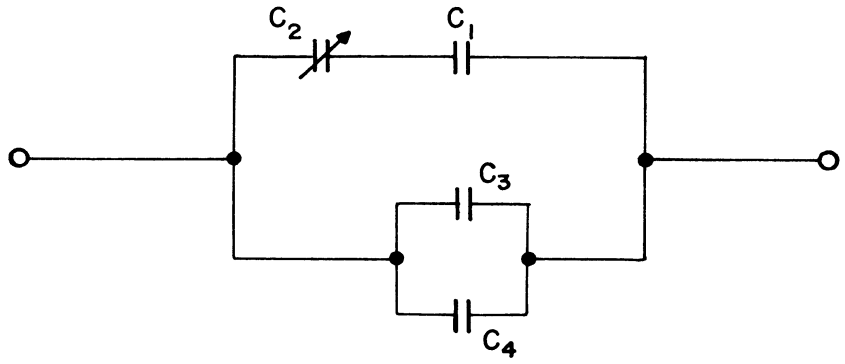

C_1 ERIE CERAMICON TUBULAR
NPO ±120 P/M 4.4μμfd ±.25μμfd

C_2 ERIE CERAMIC TRIMMER
NPO 1.5 – 7 μμ fd

C_3 POSITIVE TEMPERATURE COEF.
VITRAMON +115 P/M/°C 18μμfd
500 VDCW ±5%

C_4 NEGATIVE TEMPERATURE COEF.
CENTRALAB TCN 3.3 N750
600 VDCW ±2% 3.3μμ fd

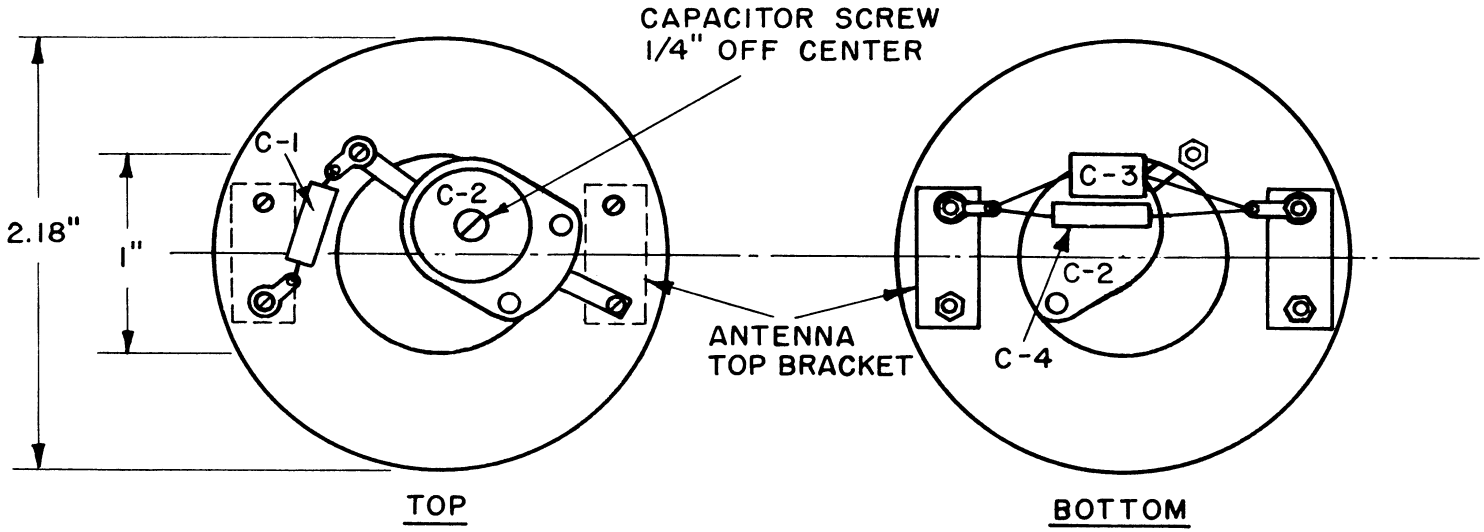

Fig. 9 Tuning Platform 37 MC Antenna

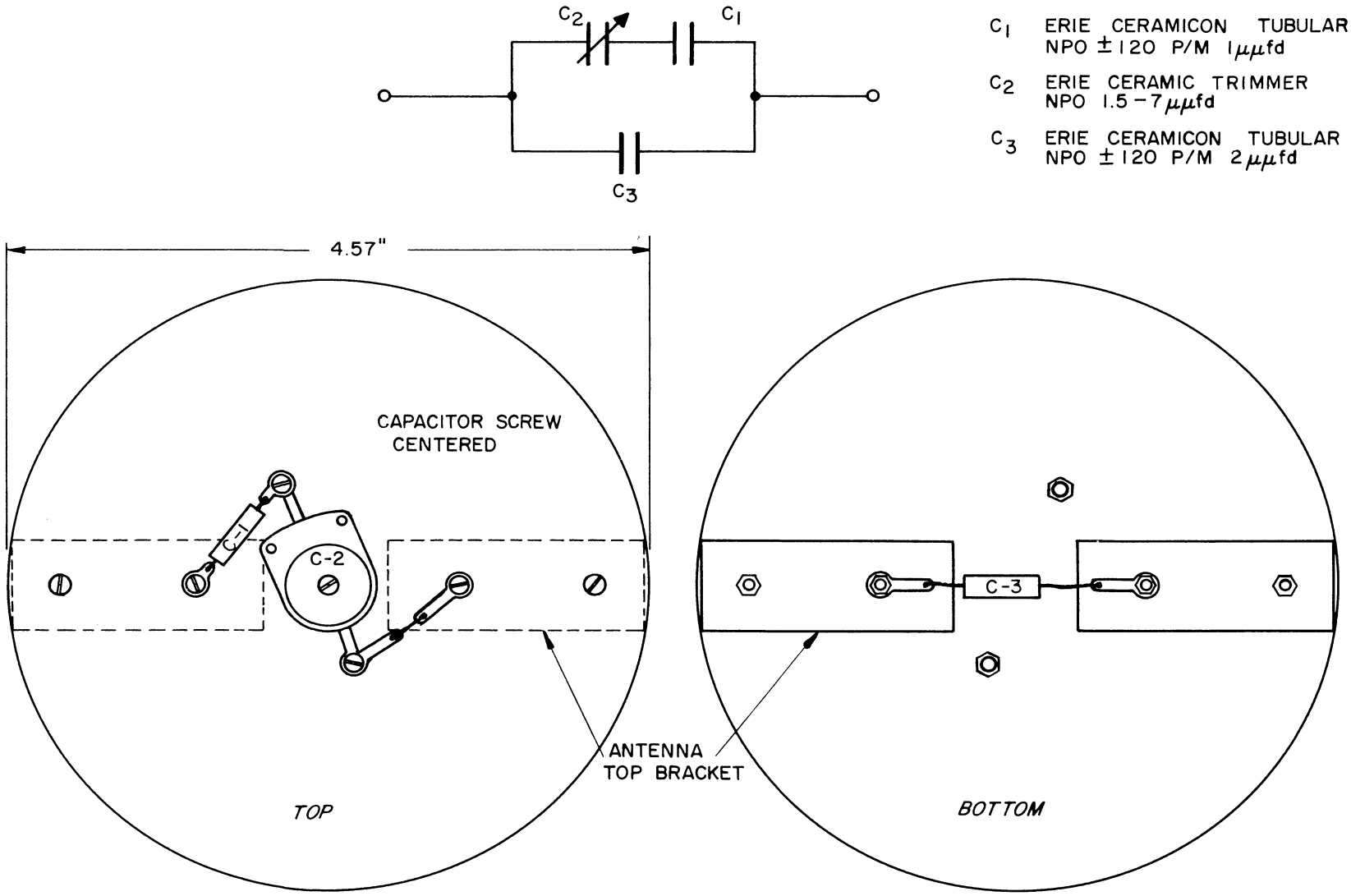

Fig. 10 Tuning Platform 148 MC Antenna

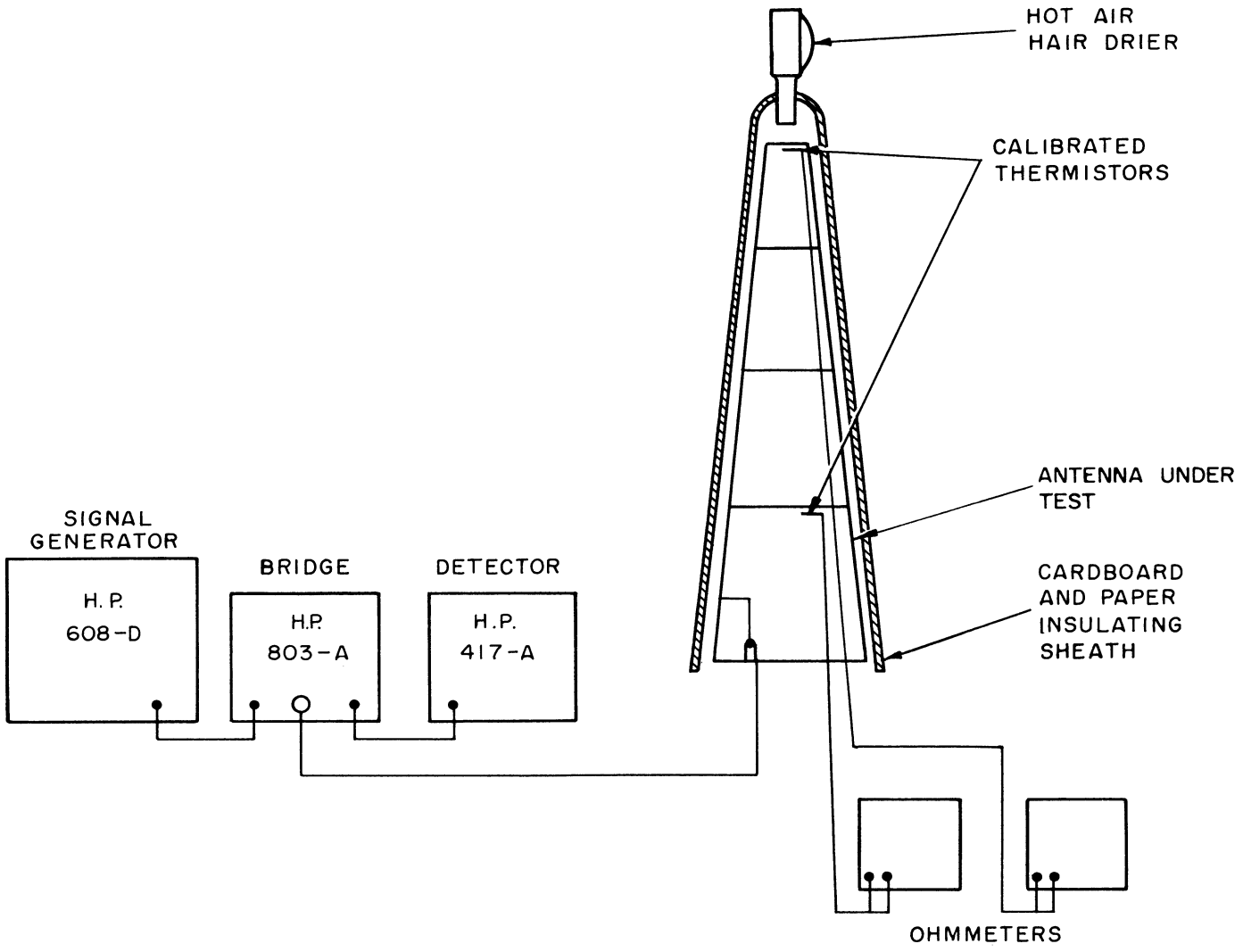

Fig. 11 Experimental Set-Up For Heat Run

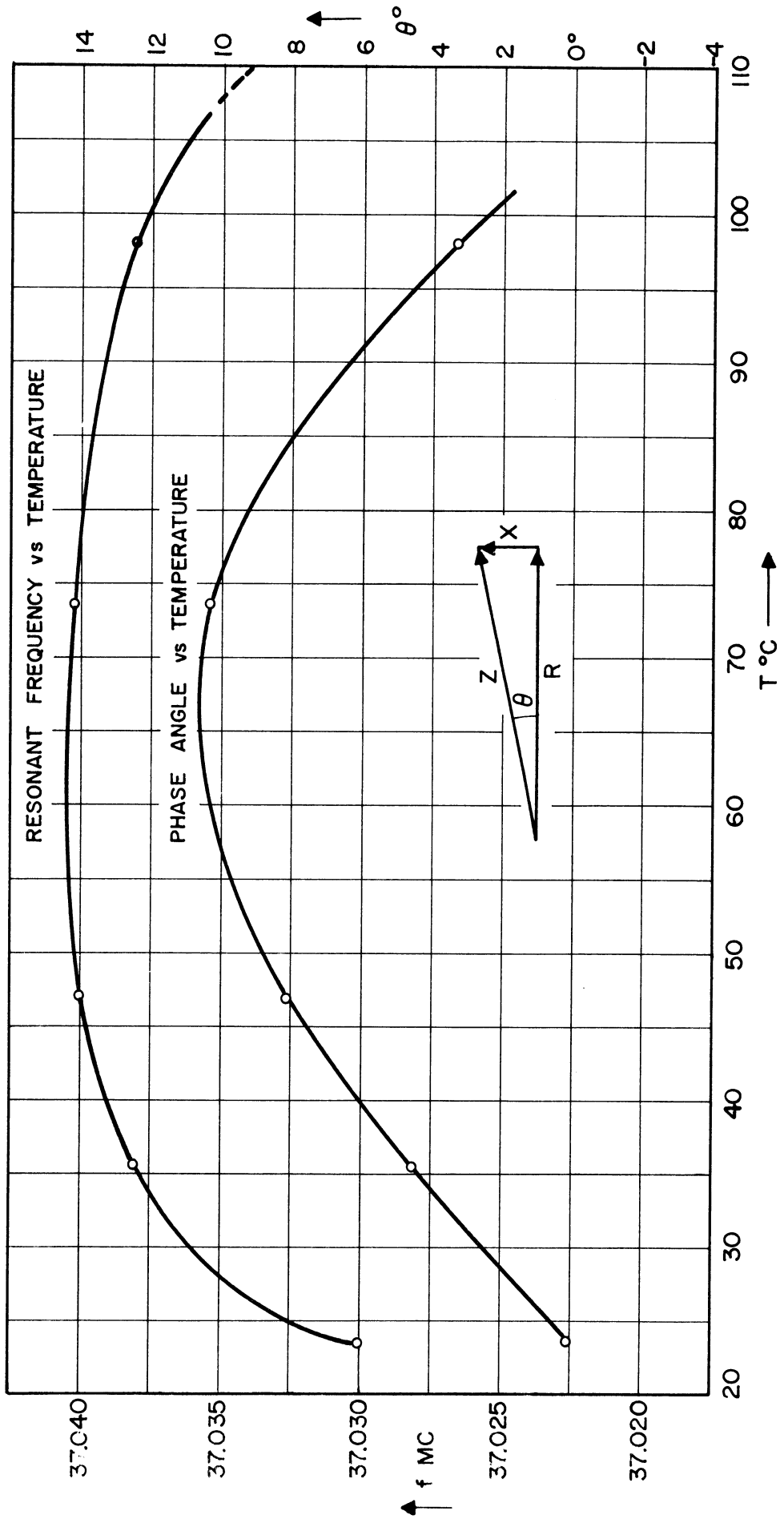

Fig. 12 Temperature Stability 37 MC Antenna

Frequency	"Q"	Tuning Range	Efficiency	Input Impedance
37 Mc	160	36.2---37.4 Mc	16 db below dipole*	50 + j0 Ω
148 Mc	50	135----160 Mc	2 db below dipole	50 + j0 Ω

In conclusion, the final antennas were made to conform to the imposed size limitations and flight expectations of the missile and at the same time meet their primary purposes electrically. The design and choice of components have proven adequate in the recent flight.

*The efficiency of the 37 Mc antenna in the flying model was never actually measured, but this figure is within one or two decibels of the true value based on accurate measurements on Antenna No. 4A. The 37 Mc unit of model No. 4A had a Q and physical dimensions almost identical with the flying models, and it showed a radiation efficiency of 15 db below dipole as reported by Mr. Victor Richard on October 8, 1959.

4. DESIGN OF BEACON TRANSMITTER

4.1. BLOCK DIAGRAM

A block diagram of the two-frequency beacon is shown in Fig. 13. It consists of the following parts:

(a) A 37 Mc crystal oscillator, powered by a separate battery.

(b) A three stage 37 Mc amplifier. The amplifier is driven by the oscillator and delivers approximately 120 mW to the antenna.

(c) Two frequency doublers and a final amplifier delivering nominally 20 mW to the 148 Mc antenna. The first frequency doubler is driven by the second stage of the 37 Mc amplifier.

(d) A telemeter generator, amplitude modulating the 148 Mc signal. The telemeter generator is a multivibrator producing a 10 msec pulse. Its repetition rate is determined by a thermistor.

(e) A Ledex stepping switch is furnished to disconnect battery power from the transmitters or to connect them to an external battery. The four positions of the Ledex correspond to the following functions:

Position 1: transmitters off.
Position 2: 37 Mc transmitter connected to the external battery.
Position 3: both transmitters connected to the external battery.
Position 4: beacon on internal battery for flight.

With this arrangement it is possible to measure the currents drawn by the two transmitters separately, as a final check before flight.

(f) A 16 volt mercury battery.

(g) Two thermistors (VECO type 32A84) are mounted in the beacon to measure the package temperature and the oscillator temperature prior to take-off.

(h) An oscillator heater (12 watts) is used to bring the oscillator case to operating temperature (47°C) and to melt part of the alloy that is used for temperature stabilization of the oscillator. This will be discussed further in Section 5.1

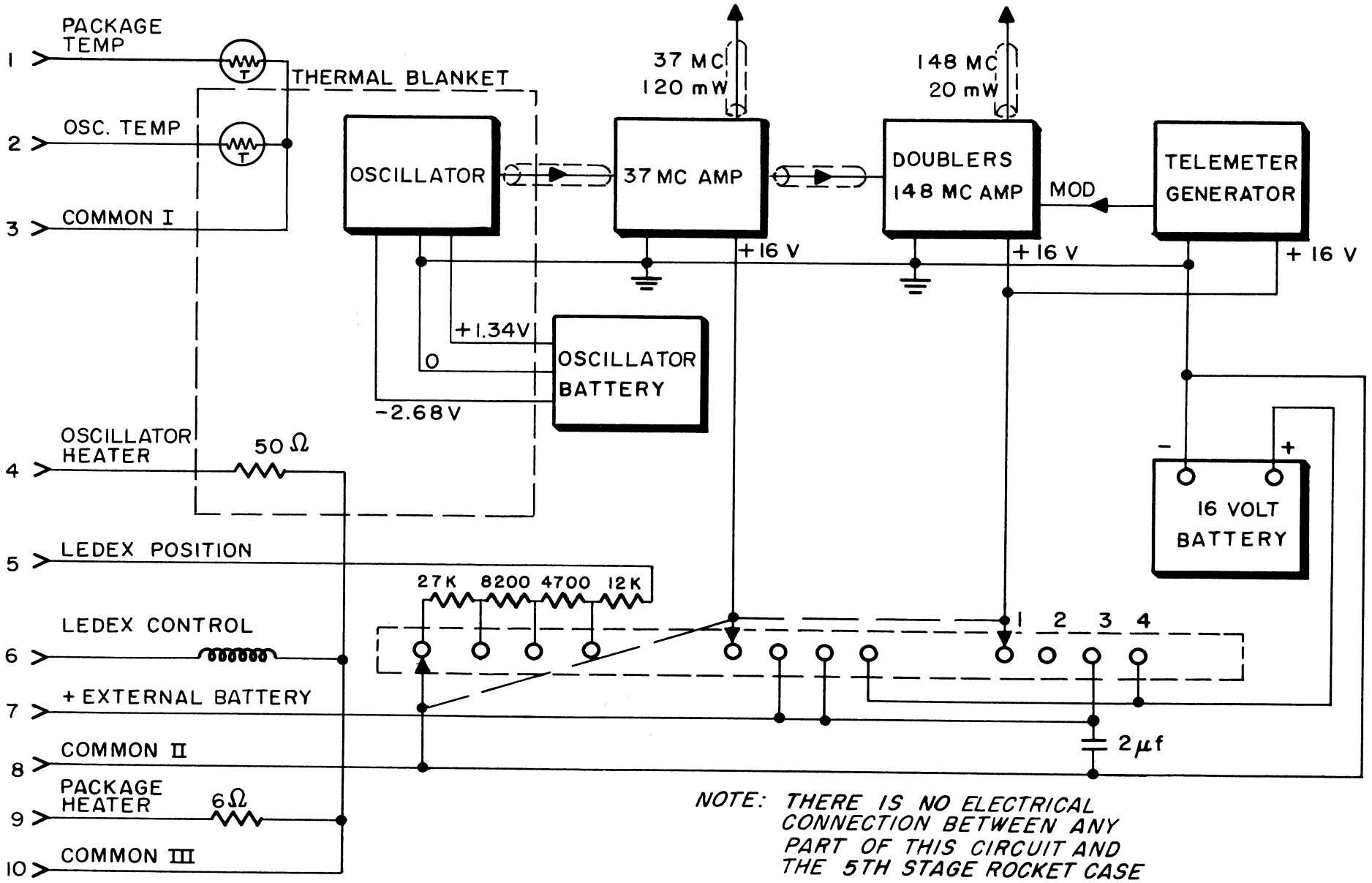

Fig. 13 Beacon Block Diagram

(i) A package heater (100 watts) is necessary to keep the package temperature above 5°C. Below this temperature the mercury batteries are not considered reliable.

The package is connected to two control panels via a 100-ft umbilical cable, a junction box on the launching pad, and a 1500-ft control cable (Fig. 14). The control panels were mounted in the BRL ground station. Figure 15 shows a diagram of the control panels. The heater control panel consists of two thermometer circuits to measure package and oscillator temperatures (see Section 5.5). The variacs on this panel furnish power to the two heaters inside the beacon. The transmitter control panel contains a power supply to operate the Ledex switch, an indicator for the position of the Ledex switch and a variable external power supply.

4.2. OSCILLATOR

The oscillator assembly is shown in Fig. 16. The mechanical and thermal design of this assembly will be discussed in Sections 4.8 and 5.1.

The oscillator circuit is shown in Fig. 17. This circuit is an improved version of a circuit originally developed by the Ballistic Research Laboratories.* The operation of this circuit can best be explained using the vector diagram shown in Fig. 18. Assuming that the phase shift in the transistor does not differ appreciably from 180°, the condition for oscillation is that the voltage OD is 180° out of phase with voltage OC, while at the same time the voltage gain in the transistor is larger than OC/OD. The phase condition will be fulfilled at a frequency ω_o, which is the series resonant frequency of the crystal. At a slightly different frequency the voltage to the base changes both in magnitude and in phase as indicated in Fig. 18 by the point D'. The faster the phase of the voltage OD changes with frequency, the more stable will be the frequency of the oscillator. It is apparent that this fast rate of change can be achieved by designing the oscillator so that the point D is as close to point O as possible. Of course the voltage gain in the transistor must always be larger than OC/OD, which is the reason that OD cannot be made arbitrarily small.

Figure 19 shows the change in frequency due to changes in the transistor bias. This is typical for the oscillator of Fig. 17.

Figure 20 shows the change in frequency due to temperature changes. The solid line indicates the frequency shift when all components of the oscillator, including the crystal, are placed in the oven. The broken line shows the frequency shift when only the crystal is heated, while the other components remain at room temperature. The slope of this latter curve represents the temperature

*Orr, L. W. and Cath, P. G., Instrumentation and Tracking of Ionosphere Probes, UMRI Report No. 2816: 3-1-P, Ann Arbor, February 1959.

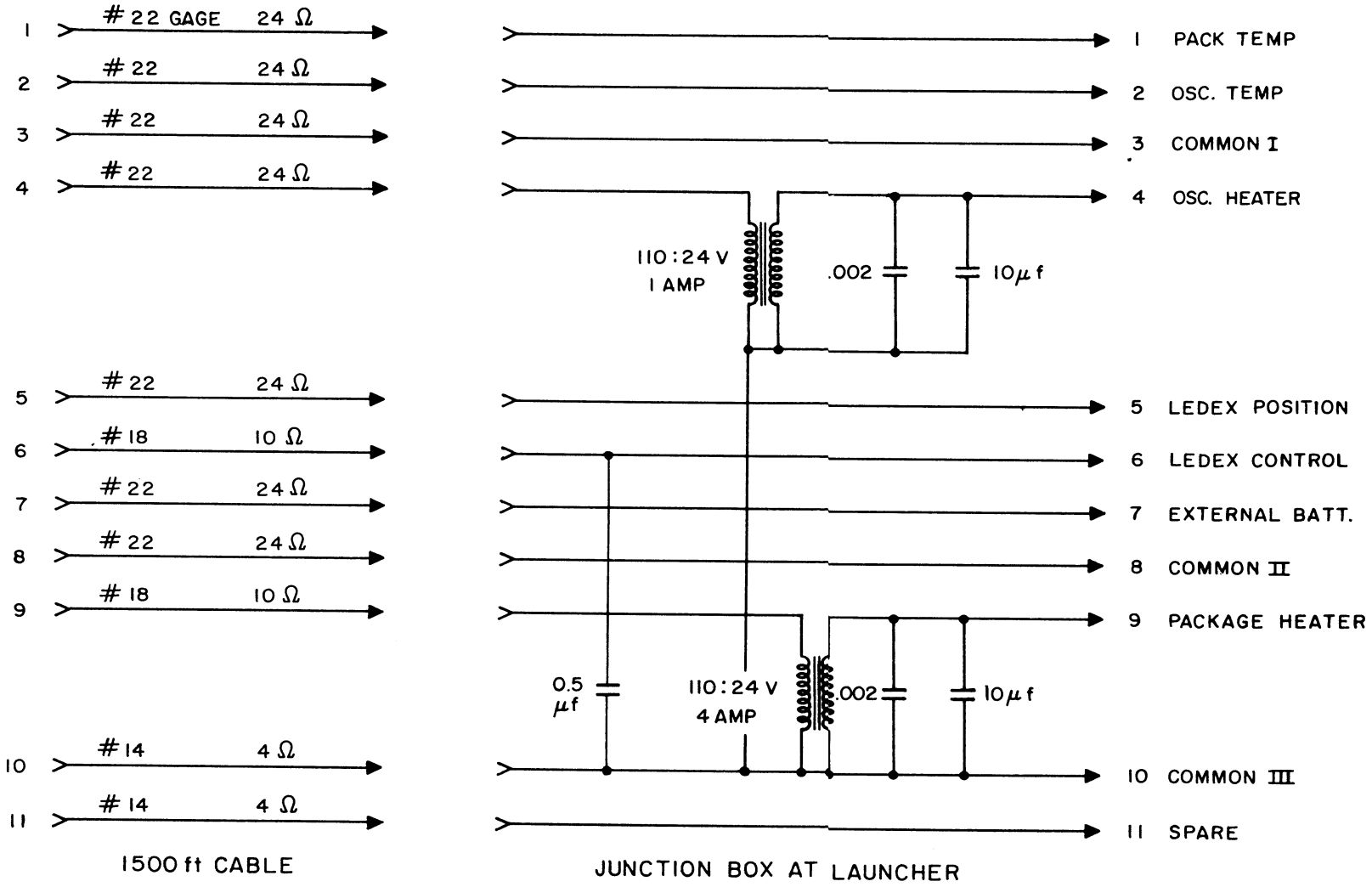

Fig. 14 Control Cable and Junction Box

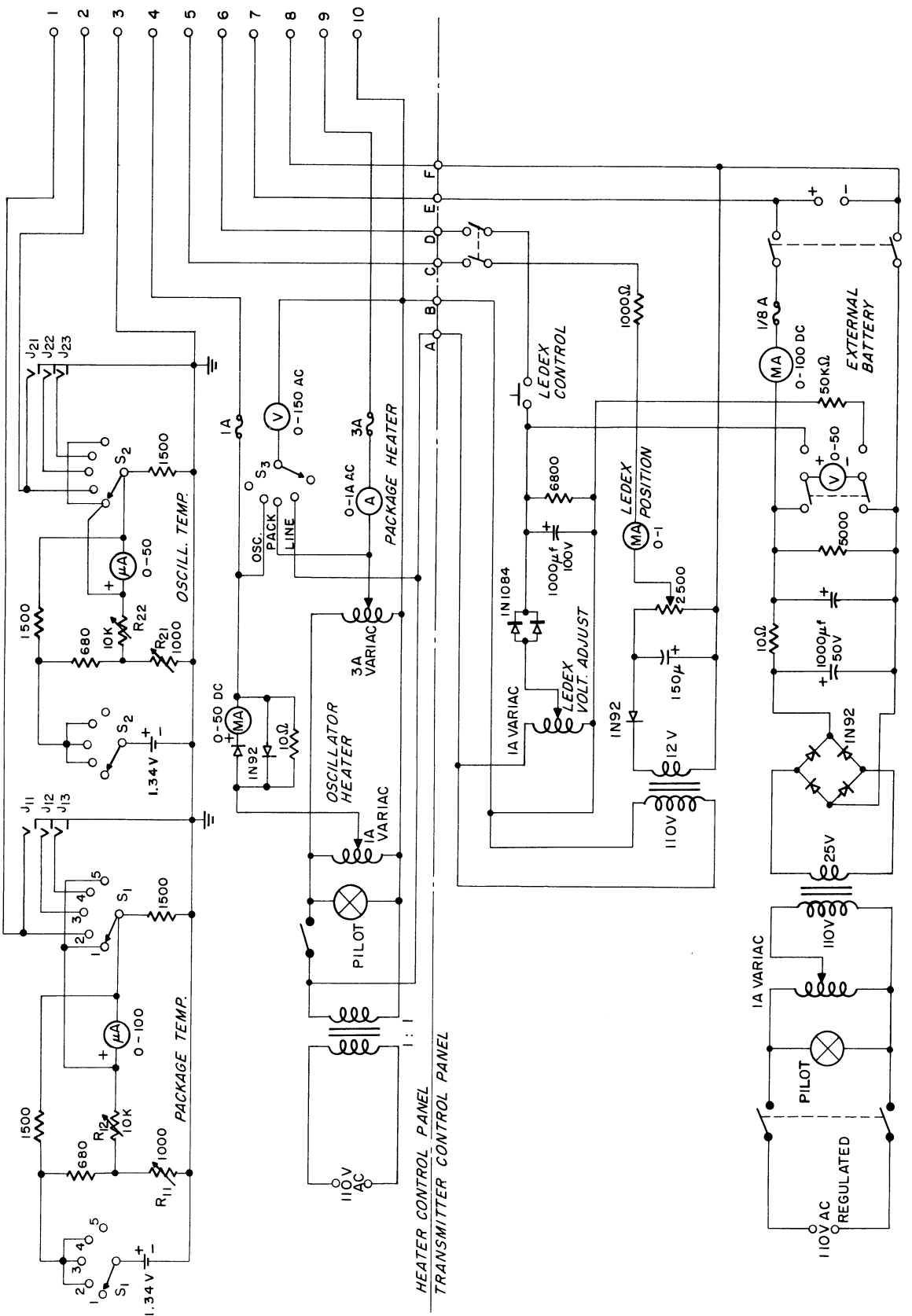

Fig. 15 Control Panels

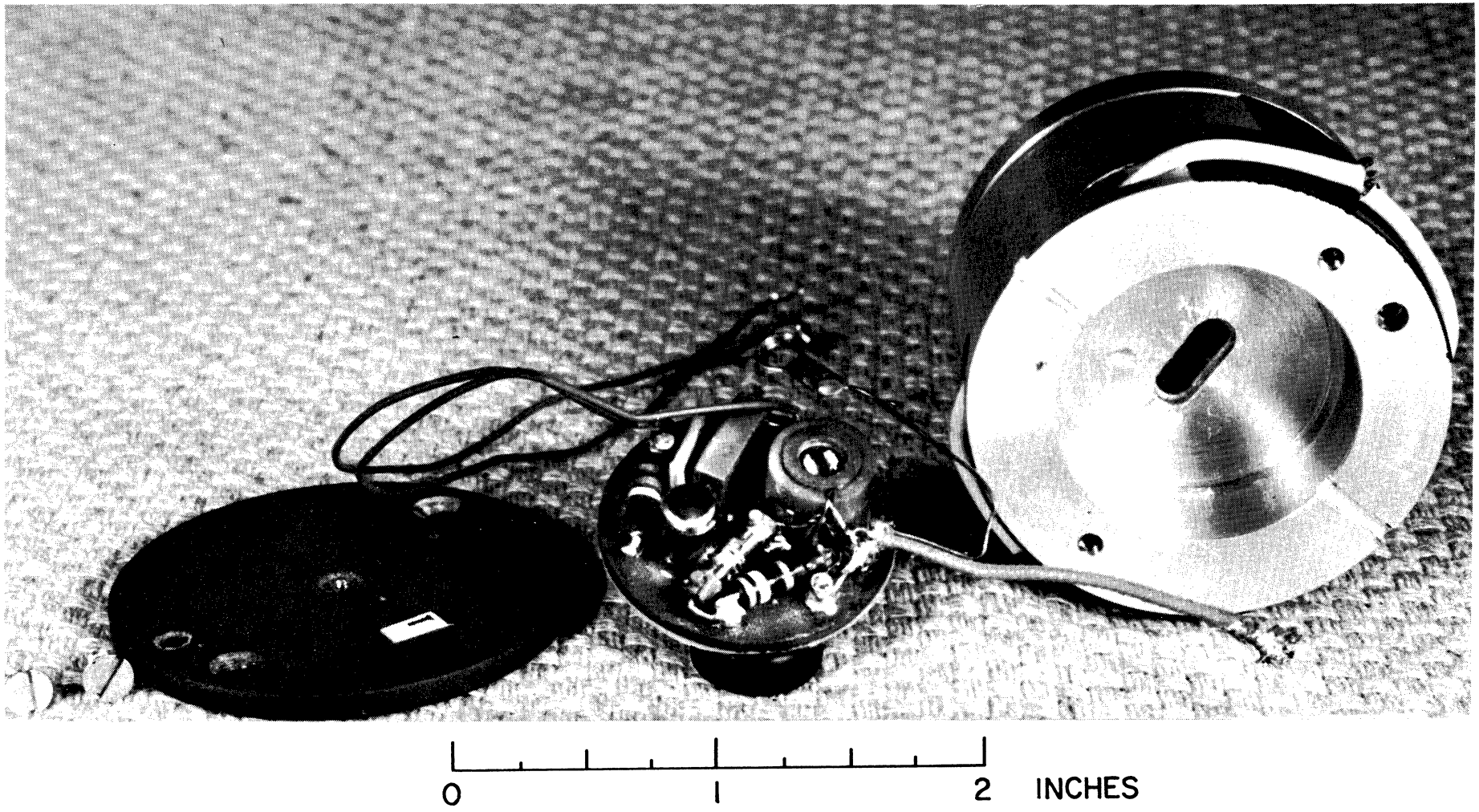

Fig. 16 Oscillator With Case

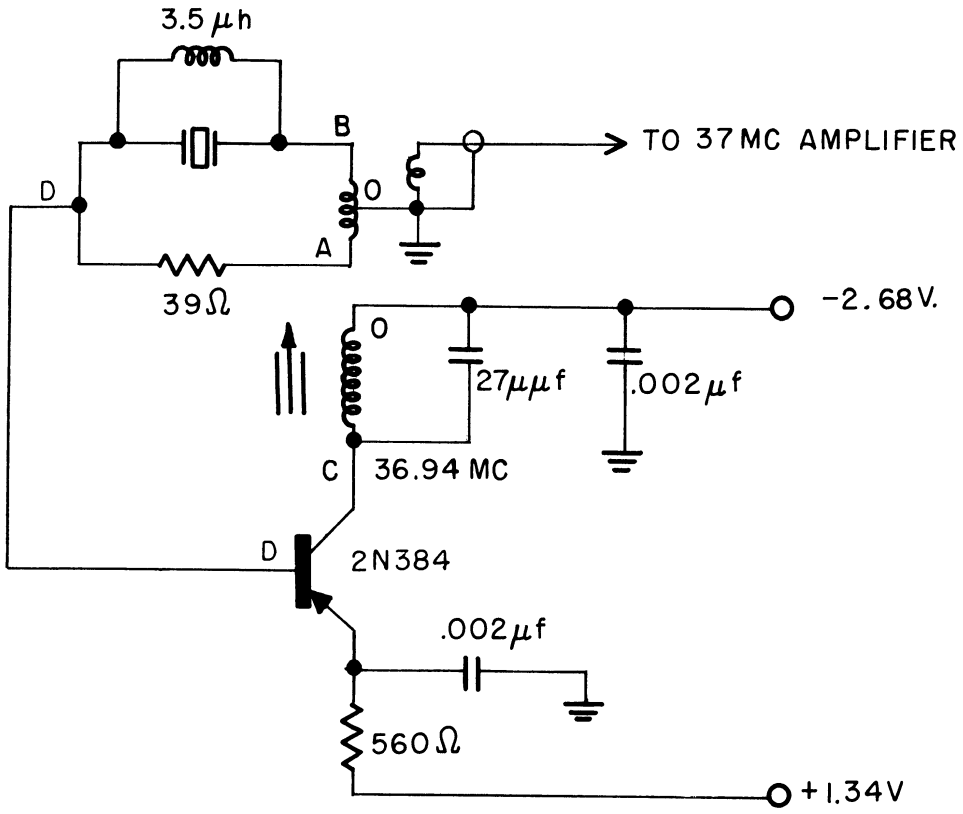

Coil data:

collector winding	7 turns
feedback winding	2 turns c.t.
output winding	1 turn

outside diameter 5/16"; # 28 enamel wire.

Fig. 17 Oscillator Circuit

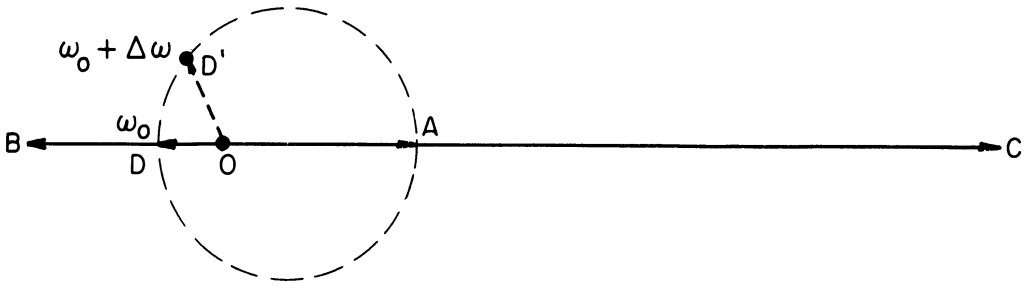

Fig. 18 Oscillator Vector Diagram

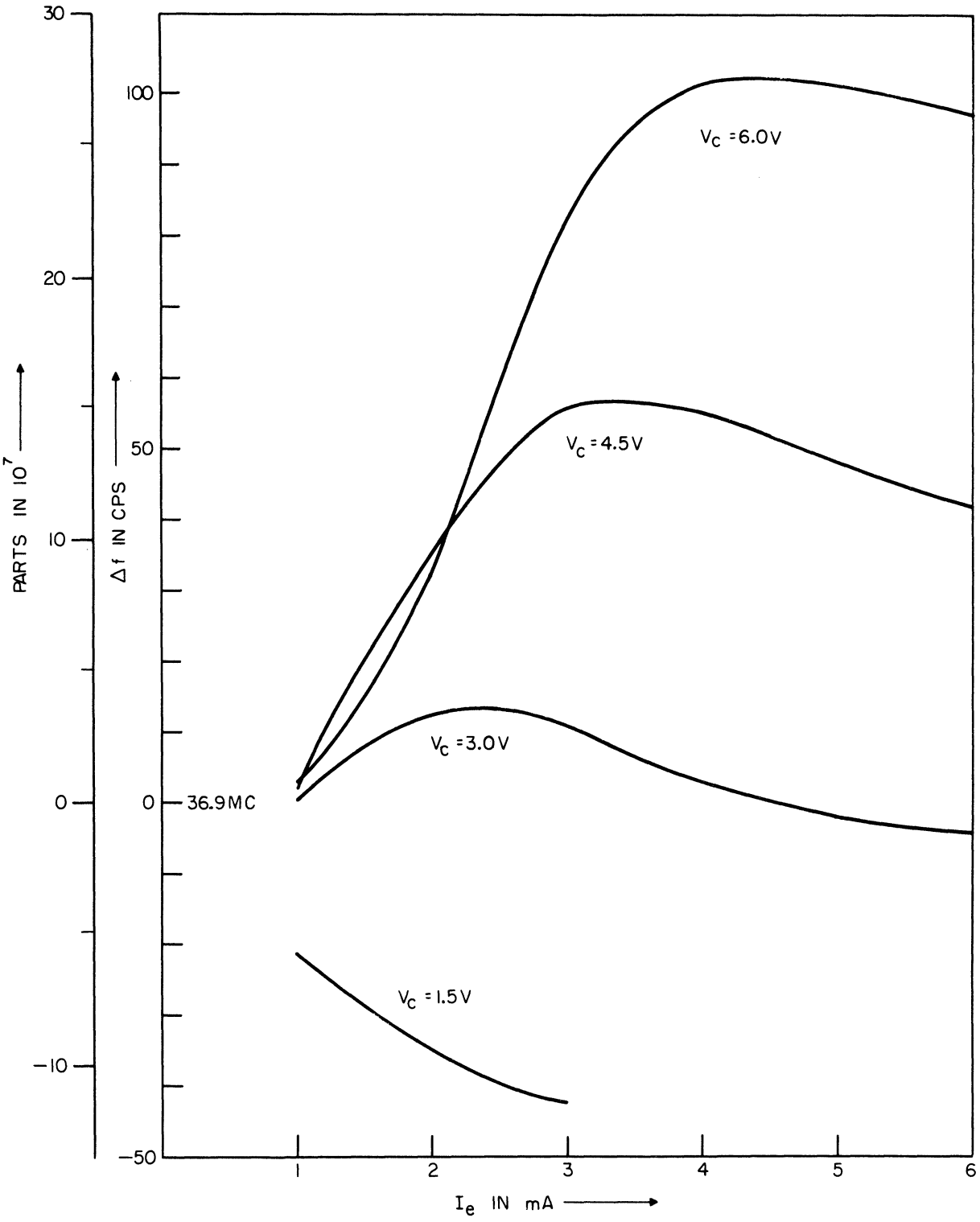

Fig. 19 Frequency Shift Due To Bias Changes

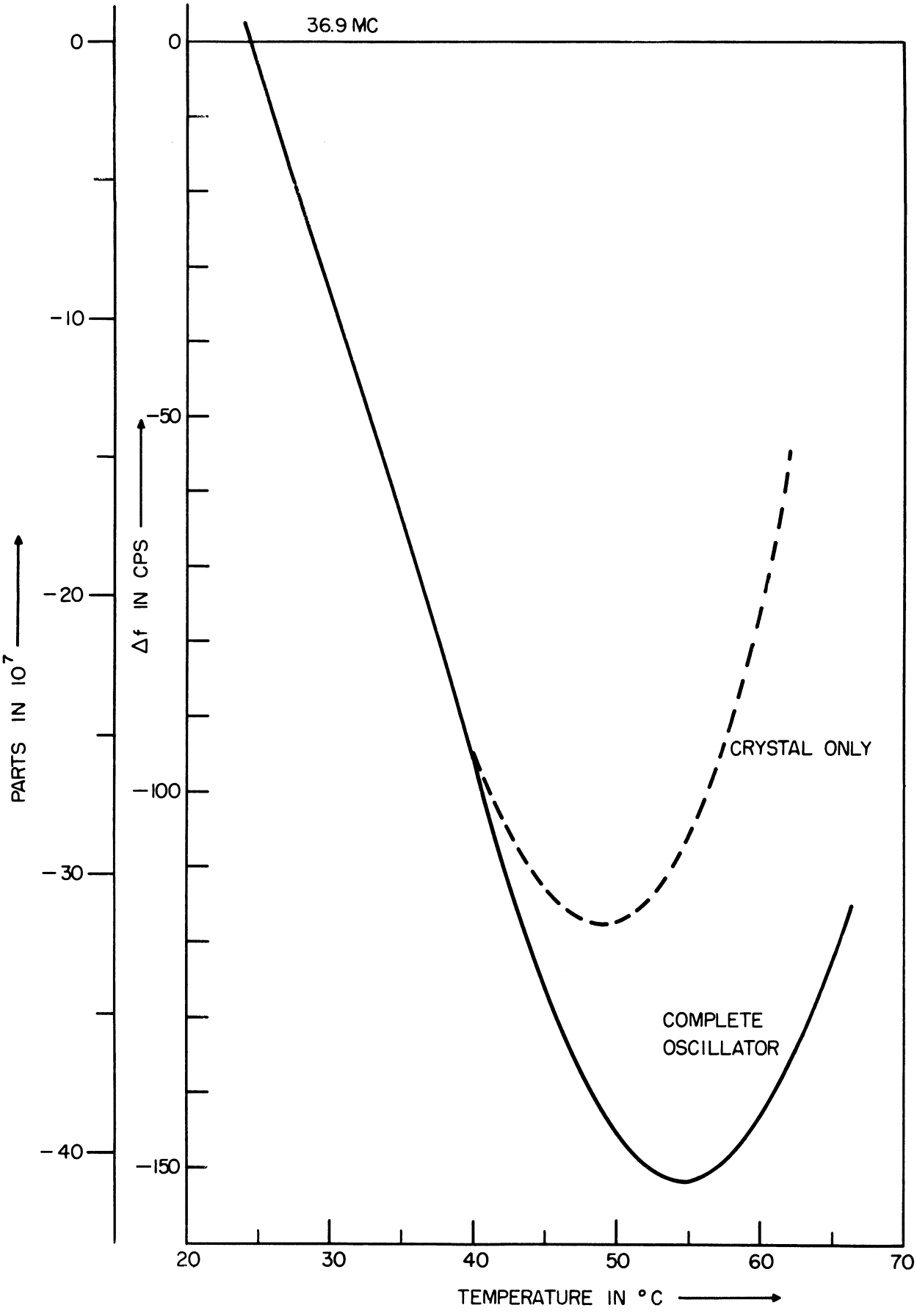

Fig. 20 Frequency Shift Due To Temperature Changes

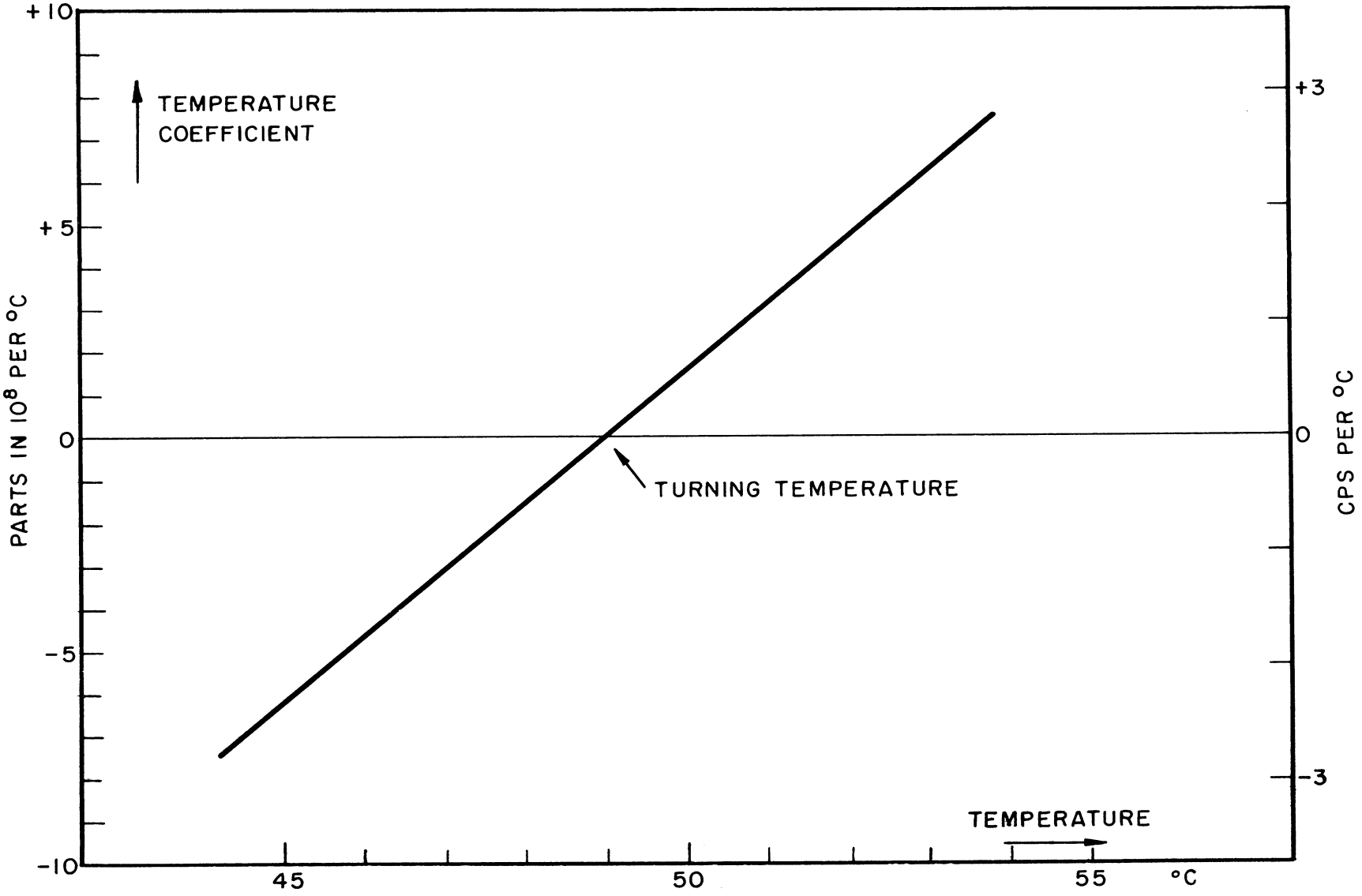

Fig. 21 Crystal Temperature Coefficient vs. Temperature

coefficient of the crystal. Figure 21 shows how the temperature coefficient varies with temperature for the crystal of Fig. 20. The crystal that was flown on November 10 had a turning temperature of 45°C and a temperature coefficient of 2.2 cycles per second per °C (or 6 parts in 10^8 per °C) at 47°C, the operating temperature.

The point at which the temperature coefficient is zero is determined by the individual crystal. It depends upon the orientation of the crystal surfaces with respect to the crystal axes. The third-harmonic crystals that are used in the oscillator are so thin, that it becomes virtually impossible to orient the crystal accurately enough during grinding, to be able still to control the temperature at which the temperature coefficient is zero. This turning temperature is therefore different for each individual unit. Fifth-harmonic crystals are much better in this respect because their larger thickness makes it easier to control the turning temperature. The disadvantage of these crystals is their larger size and higher series resistance. The more convenient third-harmonic crystals were finally used because they provided adequate frequency stability. The crystals were supplied on special order by McCoy Electronics Corporation.

4.3. DESIGN OF CLASS C OUTPUT STAGES

The main problem in the design of the 37 Mc amplifier is the output stage. In this section we shall briefly review the theoretical and practical limitations that are encountered.

The maximum power output and the efficiency of the final stage are primarily determined by the collector load. The size of this load is limited by the collector to base breakdown voltage (BV_{cbo}), the saturation voltage, and the collector dissipation.

Consider the circuit shown in Fig. 22. The peak voltage across R_L can never exceed V_b. Therefore the power delivered to R_L at the resonant frequency of the tank, can be at most

$$W_{L\ max} = \frac{V_b^2}{2R_L} .$$

W_L cannot be increased arbitrarily by increasing V_b, because of the collector-to-base breakdown voltage (BV_{cbo}). The supply voltage V_b should not exceed approximately 1/2 BV_{cbo}. Neither can W_L be arbitrarily increased by decreasing the value of R_L. When R_L is made smaller, the collector efficiency decreases and quite soon the collector dissipation becomes a limiting factor. The cause of the drop in efficiency with a decrease of R_L lies in the saturation voltage of the transistor. To be able to draw a certain value of peak current I_{cp}, a minimum collector voltage V_{cmin} is needed. The d-c admittance of the transistor under this condition can be called $\sigma = I_{cp}/V_{cmin}$.

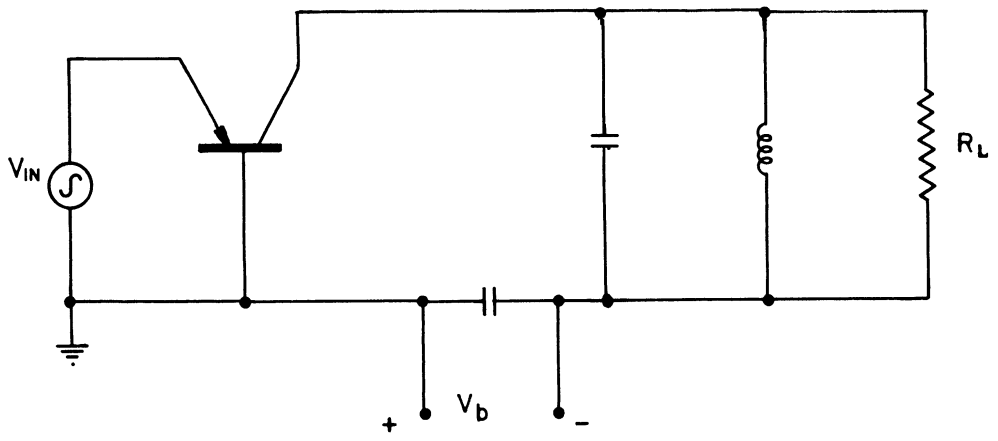

Fig. 22 Class C Output Stage

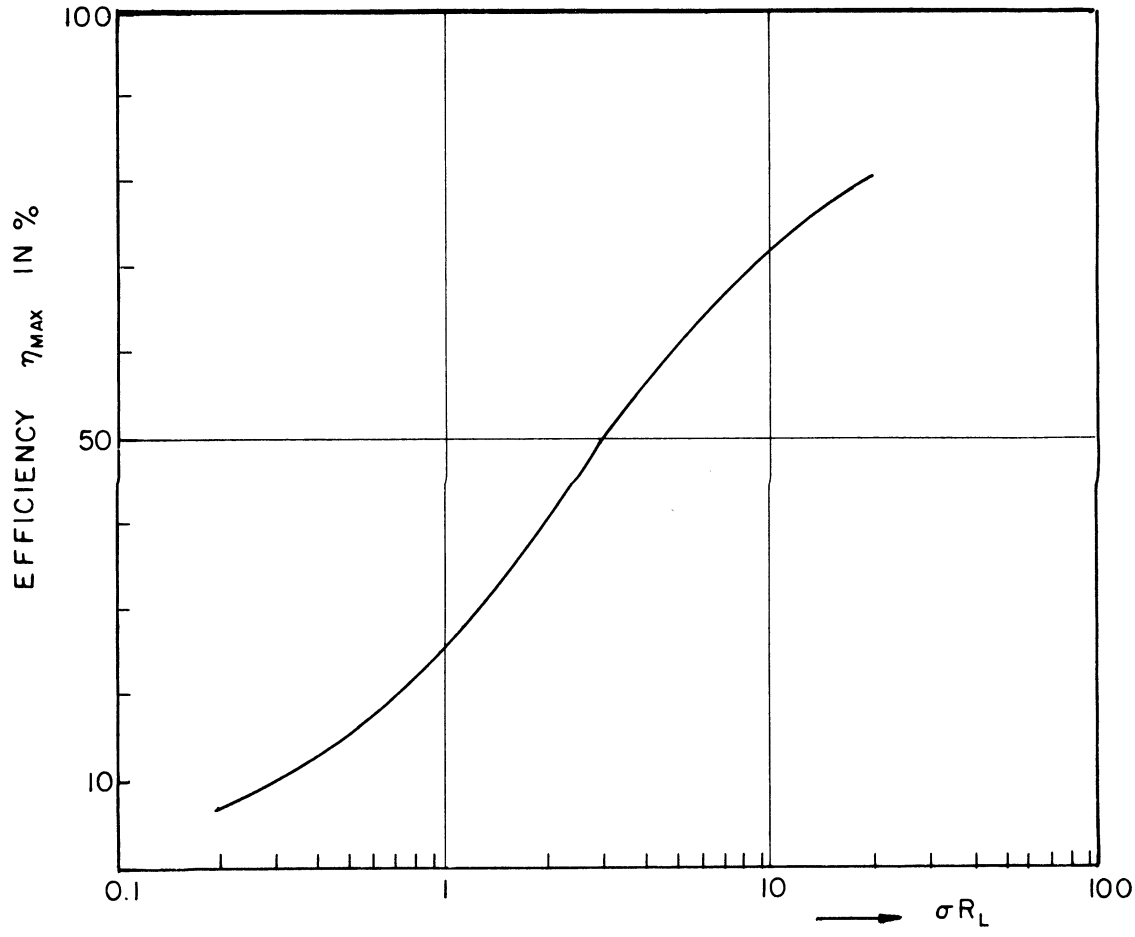

Fig. 23 Maximum Efficiency vs. Load

It can be shown that the product σR_L determines the maximum efficiency that can be obtained in class C operation.* This relationship is shown in Fig. 23. Obviously a compromise between power output and efficiency must be made when choosing a value for R_L.

Another transistor parameter that must be considered is the emitter to base reverse breakdown voltage (BV_{ebo}). This voltage is inherently low for a diffused base transistor because of the high impurity level in the base at the emitter junction. A typical value for BV_{ebo} is 0.5 - 1.0 volt. When an attempt is made to increase the output power W_L by decreasing R_L, the driving voltage to the emitter has to be increased also. This means that, during the nonconducting part of the cycle, the emitter voltage may exceed BV_{ebo}. Fortunately this breakdown is not very sharp, and it has been reported that the transistors suffer no damage when BV_{ebo} is exceeded, provided that the total emitter dissipation stays within bounds.

4.4. 37 MC POWER AMPLIFIER

Only a small amount of power is available from the oscillator for two reasons. To prevent heating of the crystal the oscillator is operated at a low power level, thus facilitating crystal temperature control. Only a small portion of this power is fed into the 37 Mc amplifier to prevent frequency pulling due to possible changes in the amplifier.

The amplifier has a power gain of approximately 500 (= 27 db) and delivers 120 mW to the 50 Ω antenna load with an overall efficiency of 35%.

The circuit diagram is shown in Fig. 24. In the first two stages 2N384 transistors are used. These are RCA drift transistors (p-n-p, alloy). A Texas Instrument 2N1143 transistor (diffused base) is used in the output stage. It is in the design of this last stage, that the considerations mentioned above have to be taken into account to obtain the desired power output at a reasonable efficiency. The tap on the output coil is adjusted so that the 50 Ω load is transformed to a load R_L = 1000 Ω at the collector. With a supply voltage of V_b = 16 volts, this stage delivers 120 mW with a collector efficiency of η = 50%. This is in good agreement with Fig. 23. The values of inductance and capacitance in the output tank are chosen to give a loaded Q of about 20. The value of Q is not critical but it should not be too high because drift in component values might otherwise detune the stage. Too low a Q gives insufficient rejection of higher harmonics.

The collector of the 2N1143 is connected to the transistor case. The transistor is therefore mounted in a small brass heat sink which is electrically insulated from the package mounting plate (Fig. 28, item 15) by a thin layer of

*Heyboer, J. P., Transmitting Valves, Philips Technical Library, Book VII, 1953.

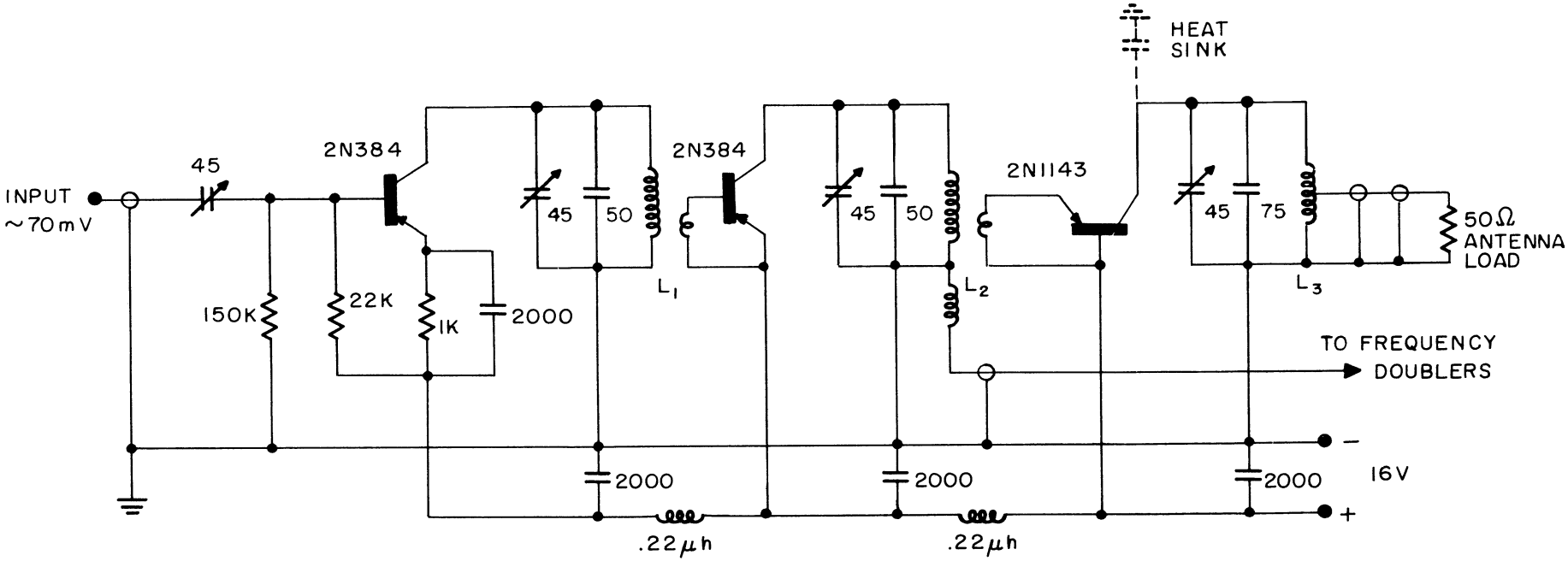

All Capacitor Values in μμf

L_1 primary 8 turns; secondary 2 turns interlaced with primary. 1/4" coil form; #20 enamel wire.

L_2 identical with L_1; third winding 5 turns #26 enamel wire.

L_3 4 turns #12 bare copper wire; tap 1 turn from end. inside diameter 1/2".

Fig. 24 37 MC Power Amplifier

teflon. Heat generated in the transistor is conducted through the teflon to the package mounting plate which also acts as a large heat sink. Teflon was chosen because it combines a reasonably good heat conductivity with a very low dielectric constant. For the dimensions used in the amplifier, the heat conductivity through the teflon layer is 76 mW/°C and the capacity added to the tank circuit by the heat sink is 8.5 μμf. The small heat sinks around the transistors are at the same time support and spacers for the amplifier mounting boards (see Fig. 28, item 2, and also Section 4.8).

4.5. FREQUENCY DOUBLERS AND 148 MC AMPLIFIER

A circuit diagram for the frequency doublers, the 148 Mc amplifier, and the telemeter generator is shown in Fig. 25.

A 37 Mc input signal to the first doubler is taken from the second stage of the 37 Mc amplifier. The frequency doubler consists of a grounded base transistor (2N1143). A diode is connected in series with the emitter to increase the second harmonic output at the collector side. Insertion of the diode decreases the portion of the RF cycle during which the transistor conducts. We believe that this accounts for the larger harmonic output at the collector. The collector tank is tuned to 74 Mc. The second frequency doubler is identical to the first. Its output tank is tuned to 148 Mc, and drives the 148 Mc amplifier.

The considerations of Section 4.3 apply of course to the collector load of the final 148 Mc stage. Because only 20 mW is required at this frequency, the tap on the output coil is adjusted so that the 50 Ω antenna load transforms into a 2000 Ω collector load to improve the efficiency.

Under certain conditions, determined by individual differences in transistor parameters, the 148 Mc transmitter oscillates. To eliminate the oscillations, damping resistors are added to the circuit as shown in Fig. 25.

Amplitude modulation of the 148 Mc signal is obtained by modulating the supply voltage to the second frequency doubler. This modulates the driving voltage to the final stage. Changing the supply voltage to the second transistor will also change the collector capacitance, which will produce some phase modulation on the 148 Mc signal. The collector capacitance however is small (1.5 μμf) compared to the fixed capacitance (approx. 10 μμf) in the tank. The amount of phase modulation is therefore small and was found not to affect the tracking filters in the ground station.

The 10-msec pulses from the telemeter generator reduce the amplitude of the 148 Mc signal by 6 db.

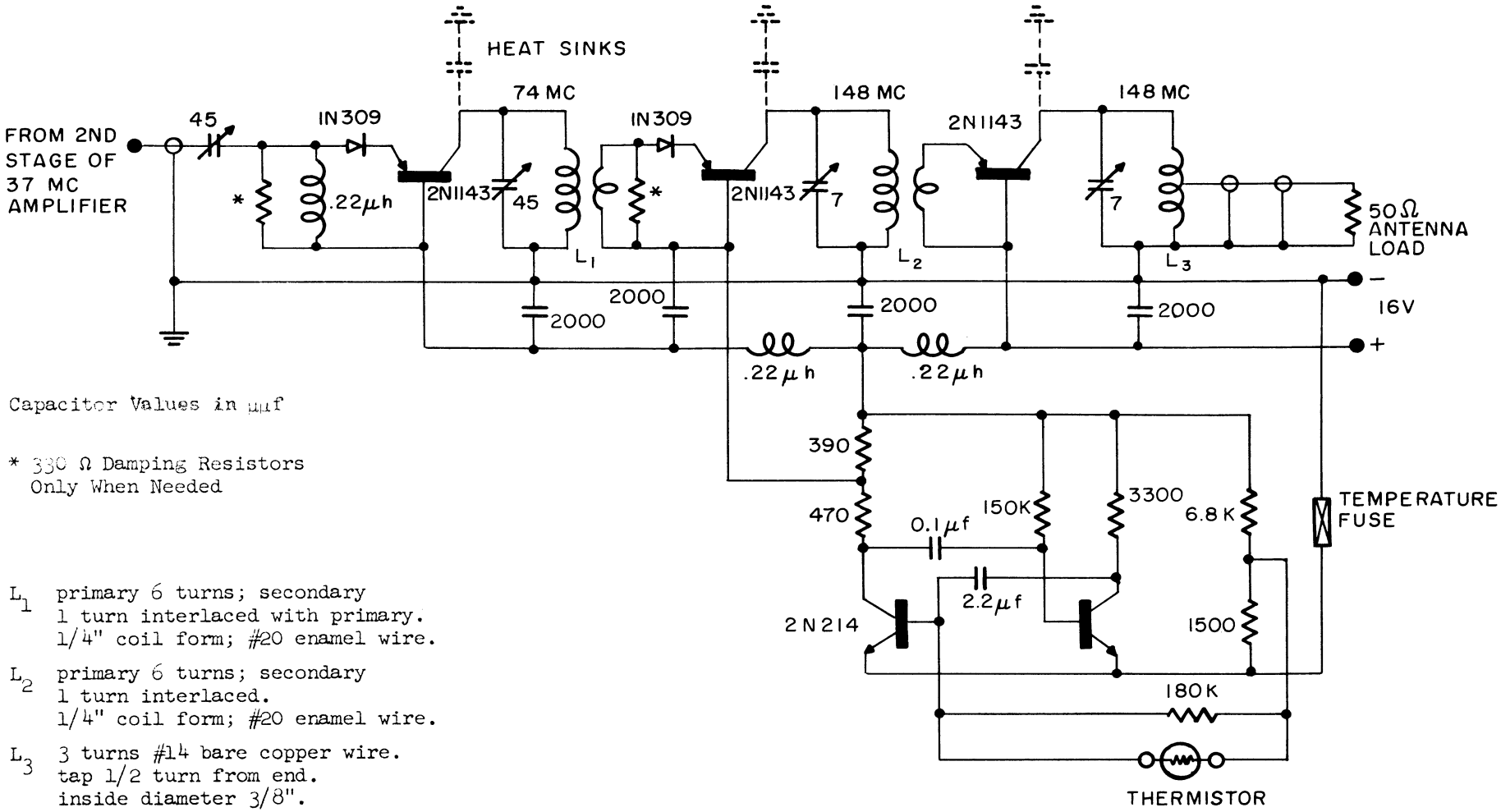

Fig. 25 148 MC Amplifier and Telemeter Generator

4.6. TELEMETER GENERATOR

At the request of the aeronautical designers, telemetry was added to the beacon for measuring the temperature at the interface of the fiberglass and teflon on the nose cone. This is probably the first measurement of its kind ever made.

The temperature of the beacon assembly itself is also of considerable interest because it determines the transistor environment.* The assembly is expected to heat up during flight, due chiefly to aerodynamic heating through the nose cone and the hot rocket case of the Scale Sergeant after burn-out. The beacon package is thermally insulated from the rocket for this reason. The third source of heat, the dissipation in the transistor circuits (about 750 milliwatt), is negligible compared to the two just mentioned.

One point on the temperature rise curve of the package was obtained using a temperature fuse. An assembly drawing of this fuse is shown in Fig. 26. The bottom stud of the fuse is screwed into the package heat sink (Fig. 28, item 15). When the package temperature reaches 47°C, the solder melts and releases the spring. This disables the telemeter generator.

The telemeter generator is a free running multivibrator. The circuit is shown in Fig. 25. N-P-N transistors are used in the multivibrator to obtain the proper polarity of output pulse for modulating the second frequency doubler by direct coupling. The pulses on the collector of the 2N214 transistors have an amplitude of 15 volts. A voltage divider (390 and 470 Ω) is used to produce the 6 volt pulses (duration 10 msec) needed to modulate the second frequency doubler. The pulse repetition rate is determined by the resistance of the thermistor (VECO type 61A7) bonded to the nose cone. Fig. 27 shows the pulse rate as a function of nose-cone temperature. The S-shape of this curve is obtained by resistances in series and in parallel with the thermistor. The series resistance consists of the 6800 and 1500 Ω resistors in the multivibrator and the parallel resistance is 180 kΩ.

4.7. BATTERY PACK

Mercury batteries were chosen for the beacon because of their constant terminal voltage throughout the useful life of the cells.

The oscillator battery consists of one 4-volt battery (Mallory type: TR133RT2). The capacity of this battery is 1000 mah, which is sufficient to

*The beacon for the second firing on November 18, was instrumented to measure the package temperature by mounting the telemeter thermistor on the package instead of the nose cone and omitting the temperature fuse. No results were obtained.

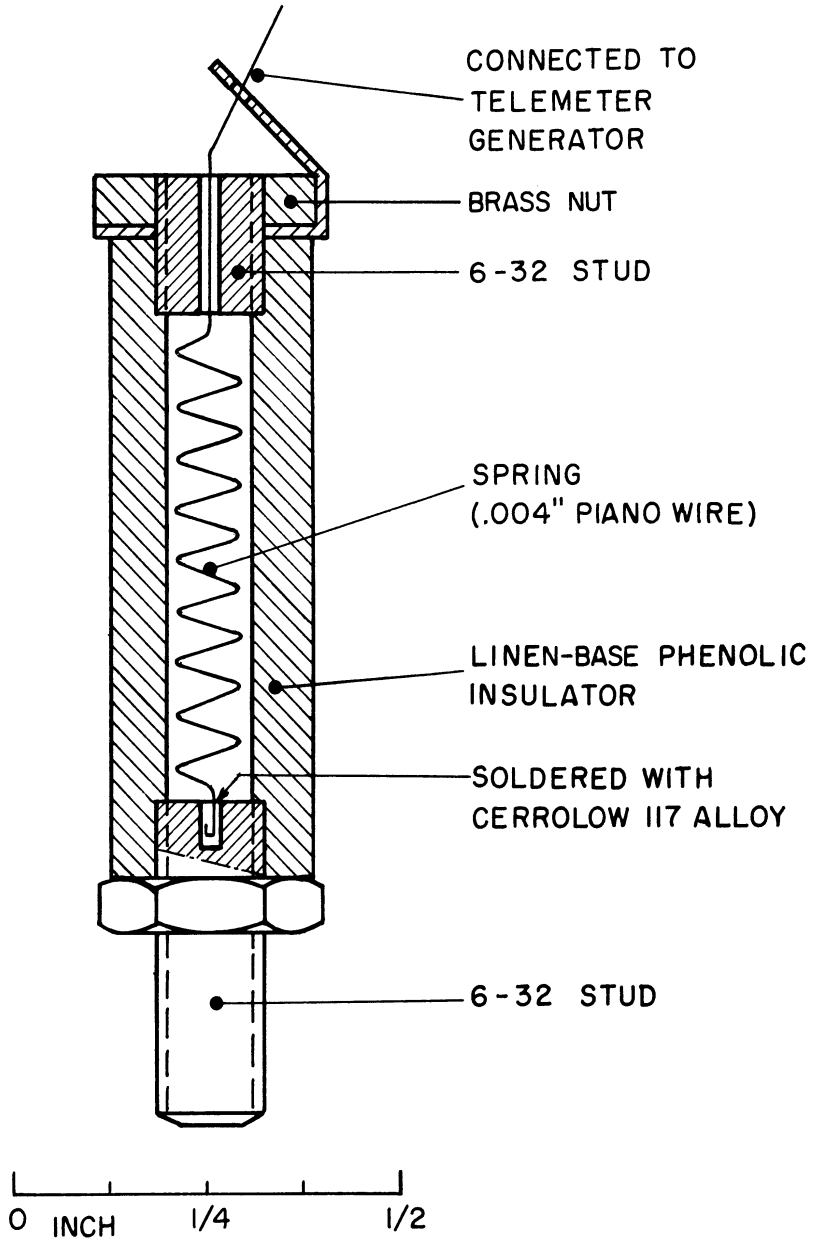

Fig. 26 Temperature Fuse

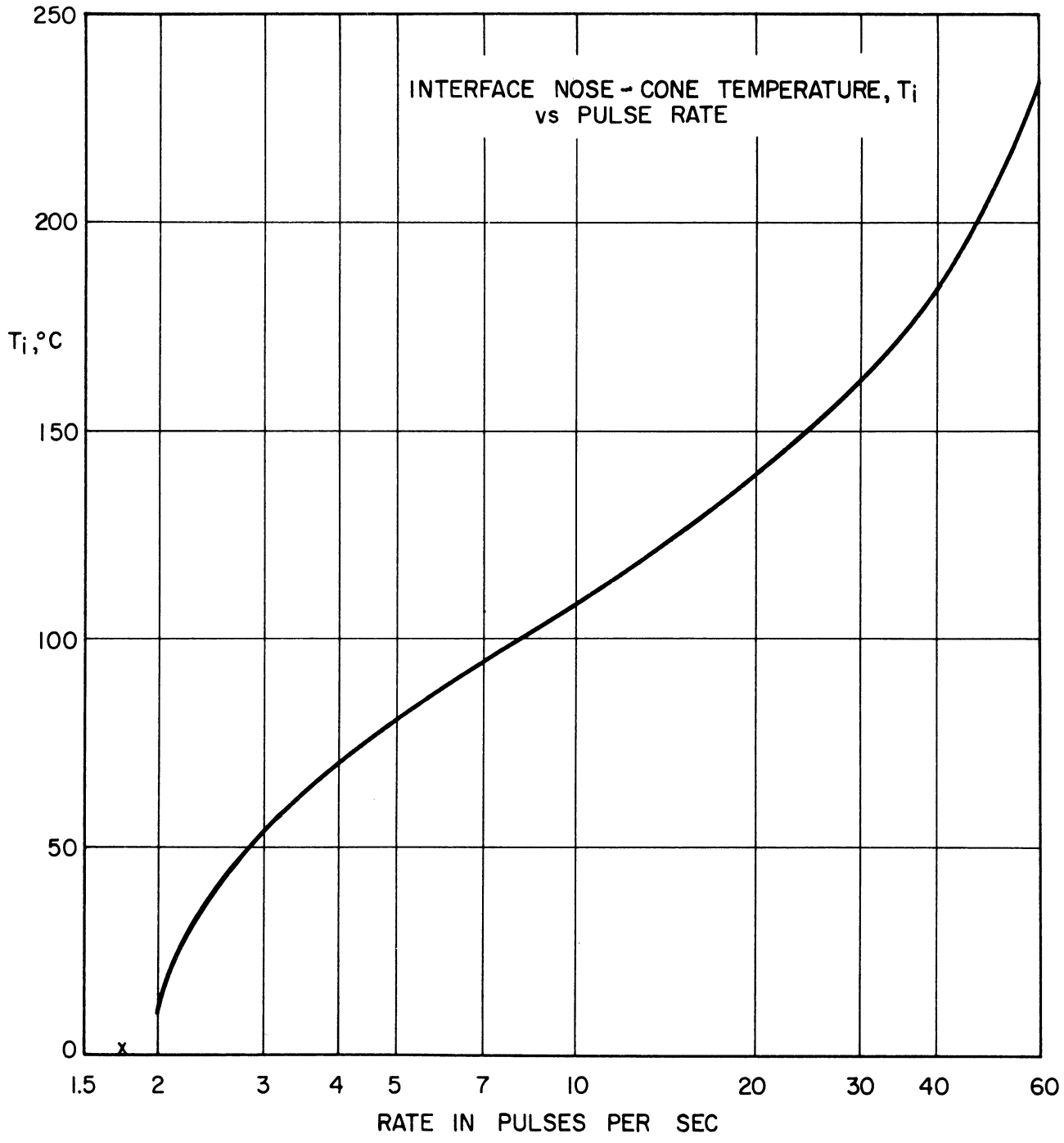

Fig. 27 Telemeter Pulse Rate vs. Nose-Cone Temperature

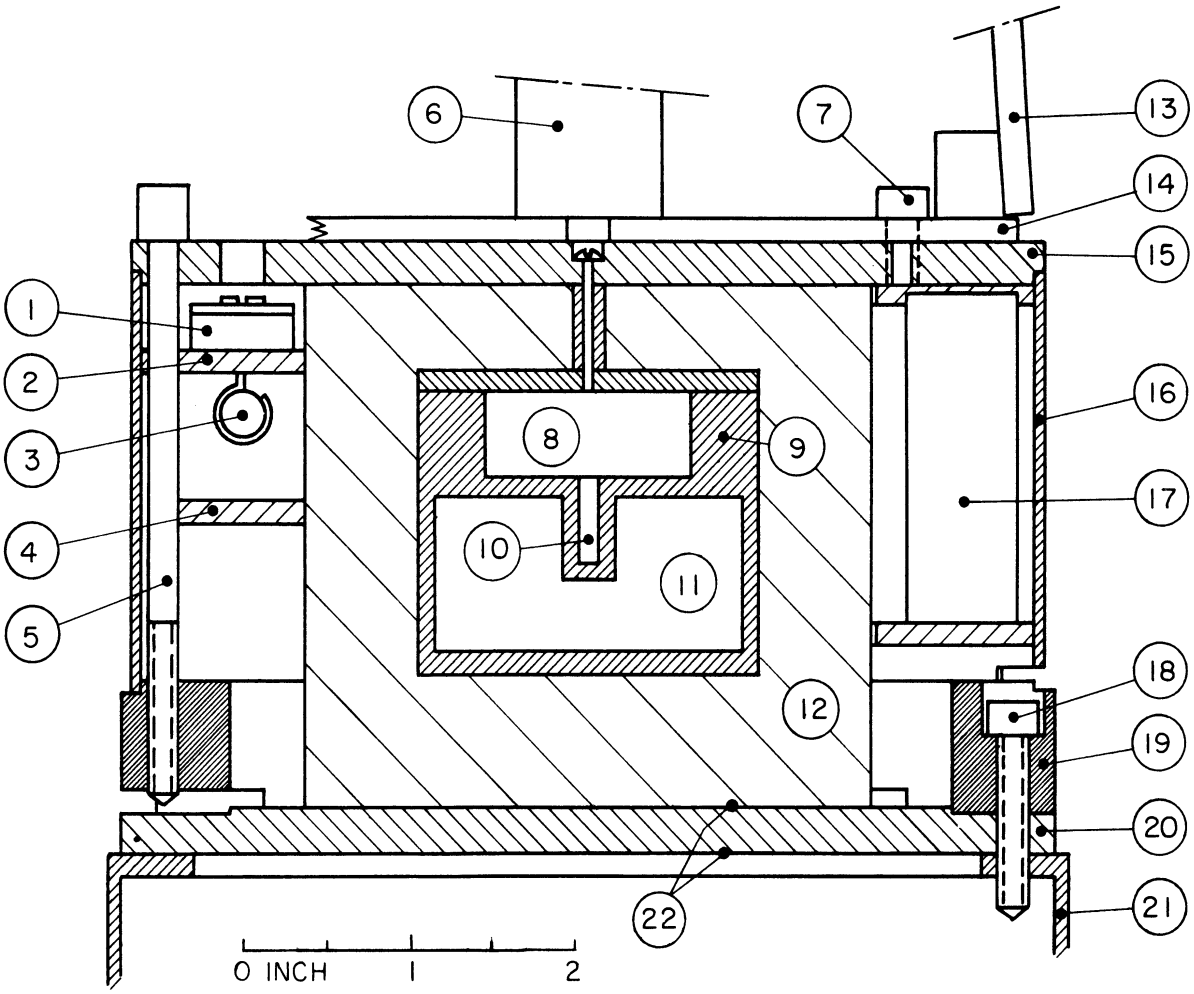

1. Tuning Capacitor
2. Amplifier Mounting Board
3. RF Coil
4. Multivibrator Mounting Board
5. Package Bolt (4)
6. Bottom of 148 MC Antenna
7. Antenna Mounting Bolt (4)
8. Oscillator Cavity
9. Oscillator Housing
10. Crystal Well
11. Cavity For Eutectic Alloy
12. Thermal Isolation Blanket
13. Bottom of 37 MC Antenna
14. Antenna Base Plate
15. Mounting Plate and Heat Sink
16. Aluminum Cylinder and Support
17. Battery Pack
18. Mounting Bolt (8)
19. Glass-Fibre Ring (G-5)
20. Teflon Plate
21. Mounting Shoulder of Scale Sergeant
22. Aluminum Foil Radiation Shields.

Fig. 28 Package Assembly Drawing

power the oscillator for 500 hours. The oscillator can therefore be connected 10 days or more before the firing. The 16-volt battery which powers the transmitter circuits, is made up of four 4-volt mercury batteries (Mallory type: TR133RT2). Its capacity is sufficient for at least 16 hours of continuous operation.

These five batteries are assembled to form one battery pack. This pack is mounted on the package mounting plate (Fig. 28, item 15) with three bolts. This facilitates replacement by fresh batteries prior to flight.

4.8. CONSTRUCTIONAL DETAILS

The most important mechanical features of the beacon assembly are shown in Fig. 28. The chief member of the assembly is the package mounting plate and heat sink (item 15). All components, oscillators, amplifiers, batteries, etc., are mounted on the bottom of this plate. The antenna is mounted on top. The mounting plate is supported by a cylindrical aluminum shell (item 16) and mounted on a glass-fibre ring (item 19) with bolts (item 5). The glass-fibre ring and the teflon plate (item 20) provide the thermal insulation between the package and the rocket case (item 21).

The oscillator case contains two cavities. The oscillator circuit is mounted in the upper one (item 8) with the crystal fitting in the crystal well (item 10) (compare Fig. 16). The other cavity (item 11) is filled with Cerrolow 117, which is the alloy used for temperature control of the oscillator (see Section 5.1). The oscillator case is surrounded by an insulating plastic foam blanket* (item 12). The other components of the beacon are placed around the oscillator (Figs. 29, 30, and 31).

Figure 29 shows a close-up of the 37 Mc amplifier. This whole amplifier section can easily be removed by removing the four mounting screws, two of which can be seen. Next to the last mounting screw the small heat sink is visible, that fits over the transistor case. This heat sink is electrically insulated from the package mounting plate by a square piece of teflon. The heat sink acts as support and spacer for the 37 Mc amplifier mounting board. The tuning capacitors (Fig. 28, item 1) are mounted on this board and can be tuned through holes in the package mounting plate.

Figure 30 shows a close-up of the 148 Mc transmitter and the telemeter generator. The same construction is used for this section, with the transistor heat sinks acting as spacers and supports for the mounting board.

To withstand flight conditions the amplifier components are surrounded by plastic foam*. A foamed-in package ready for flight is shown in Fig. 31. Notice also the package heater mounted on the aluminum shell, consisting of several

*E-P-Fome with 270 catalyst. Electronic Plastics Corporation, New York.

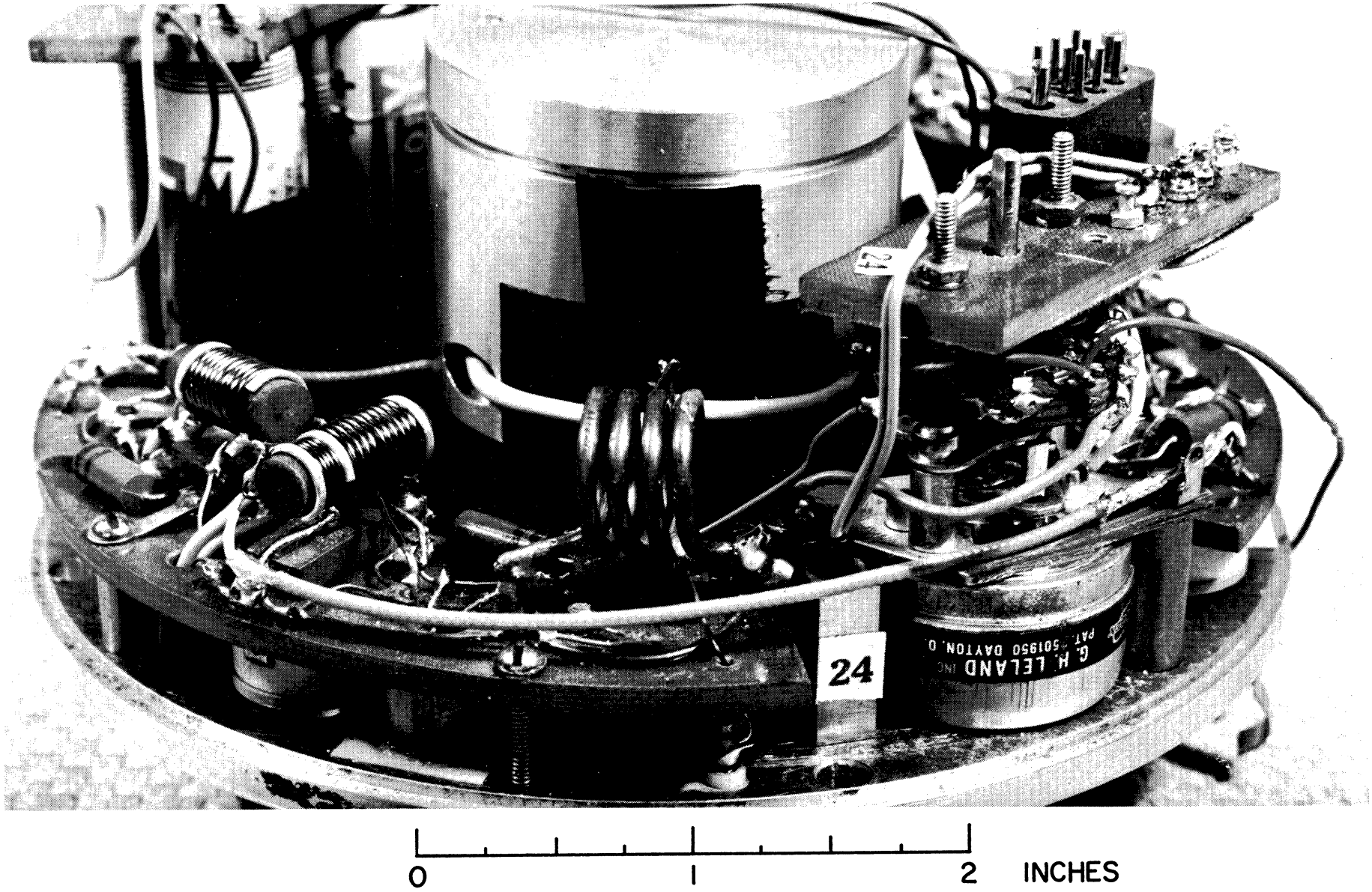

Fig. 29 View of 37 MC Amplifier

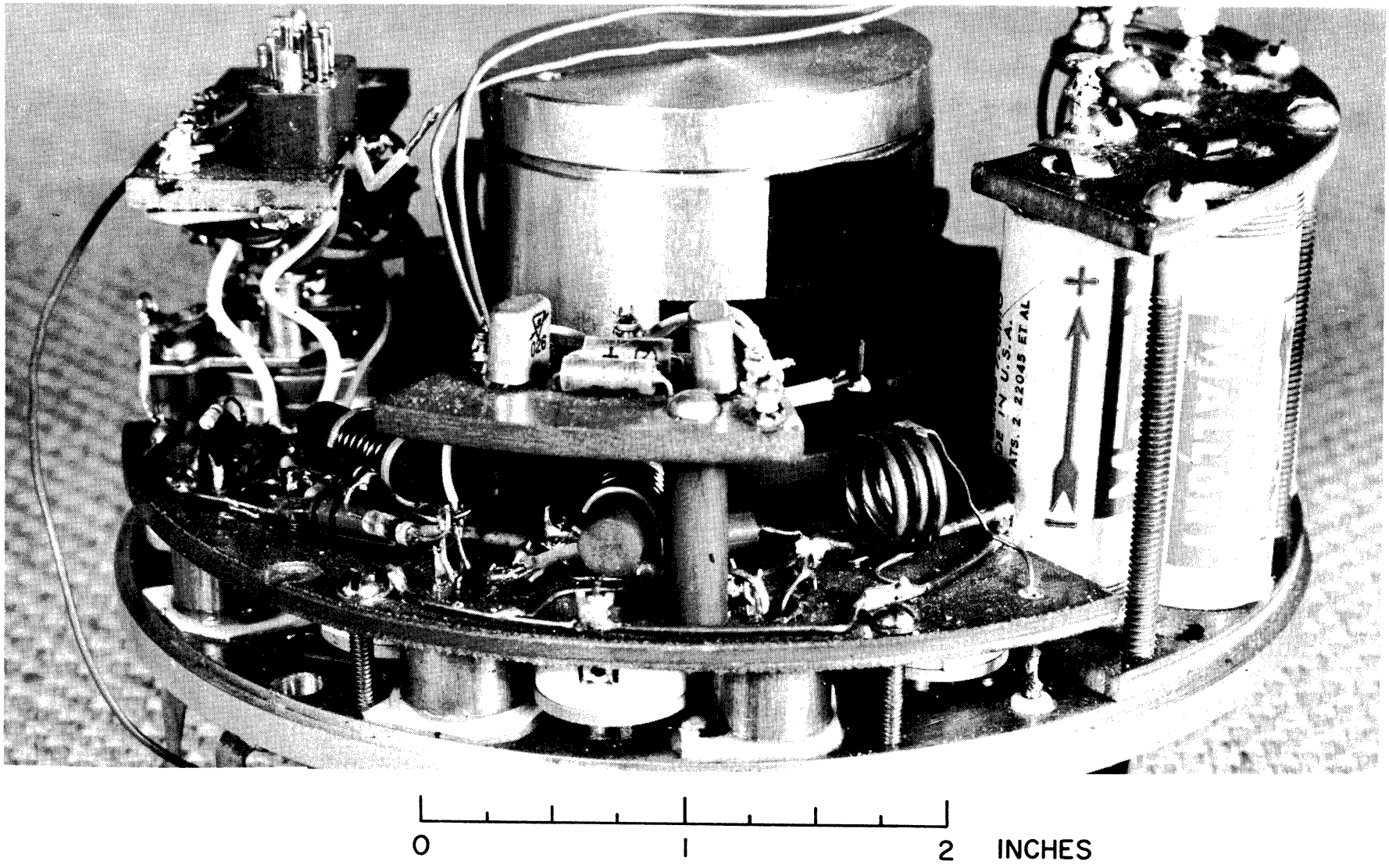

Fig. 30 View of 148 MC Amplifier and Telemeter Generator

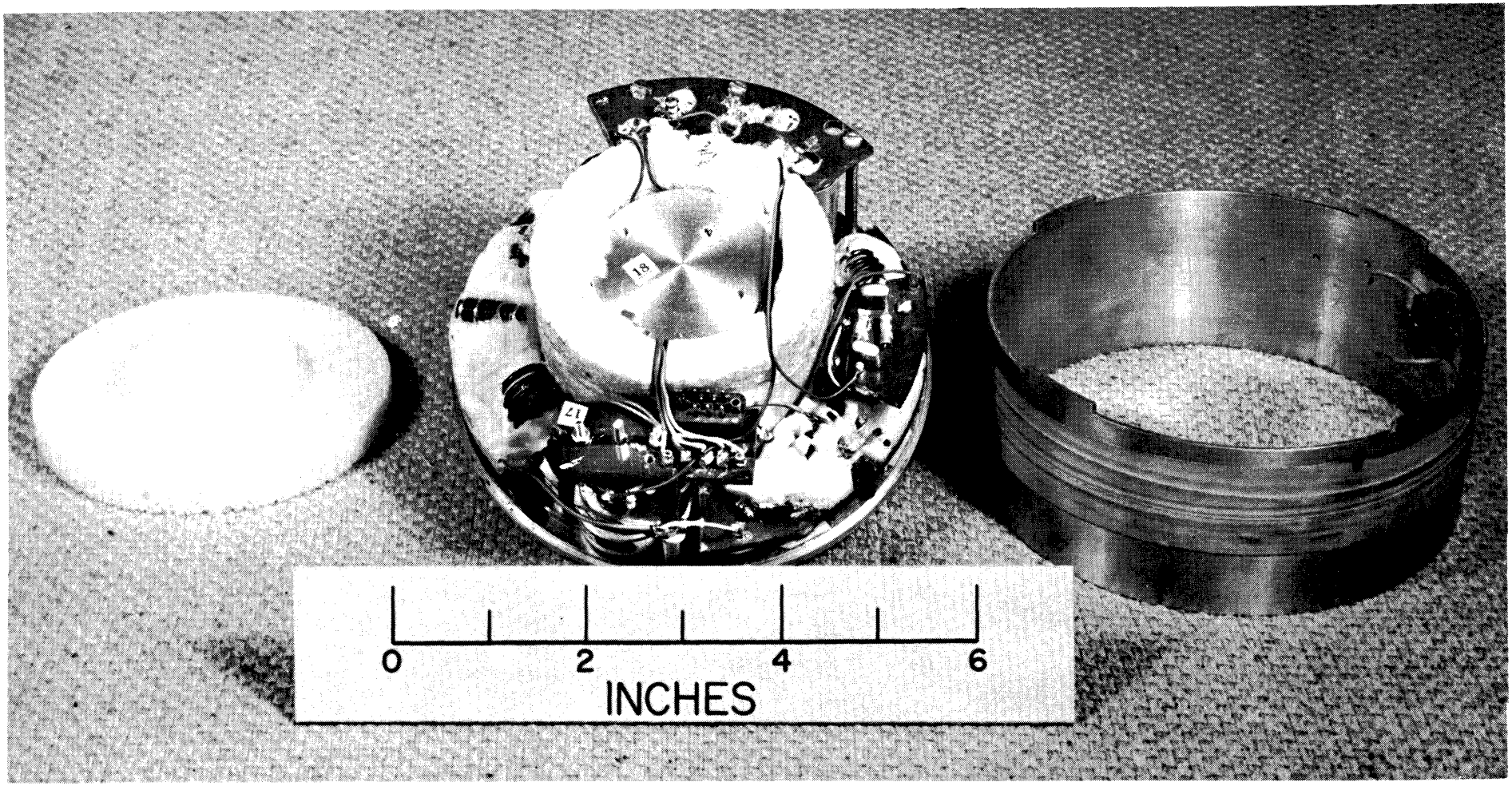

Fig. 31 Beacon Assembly Completed With Foam

turns of resistance wire taped to the outer surface.

A photograph of the beacon completely assembled, and the base of the antenna is shown in Fig. 32. Two spring contacts on top of the package are provided to make contact with the nose-cone thermistor.

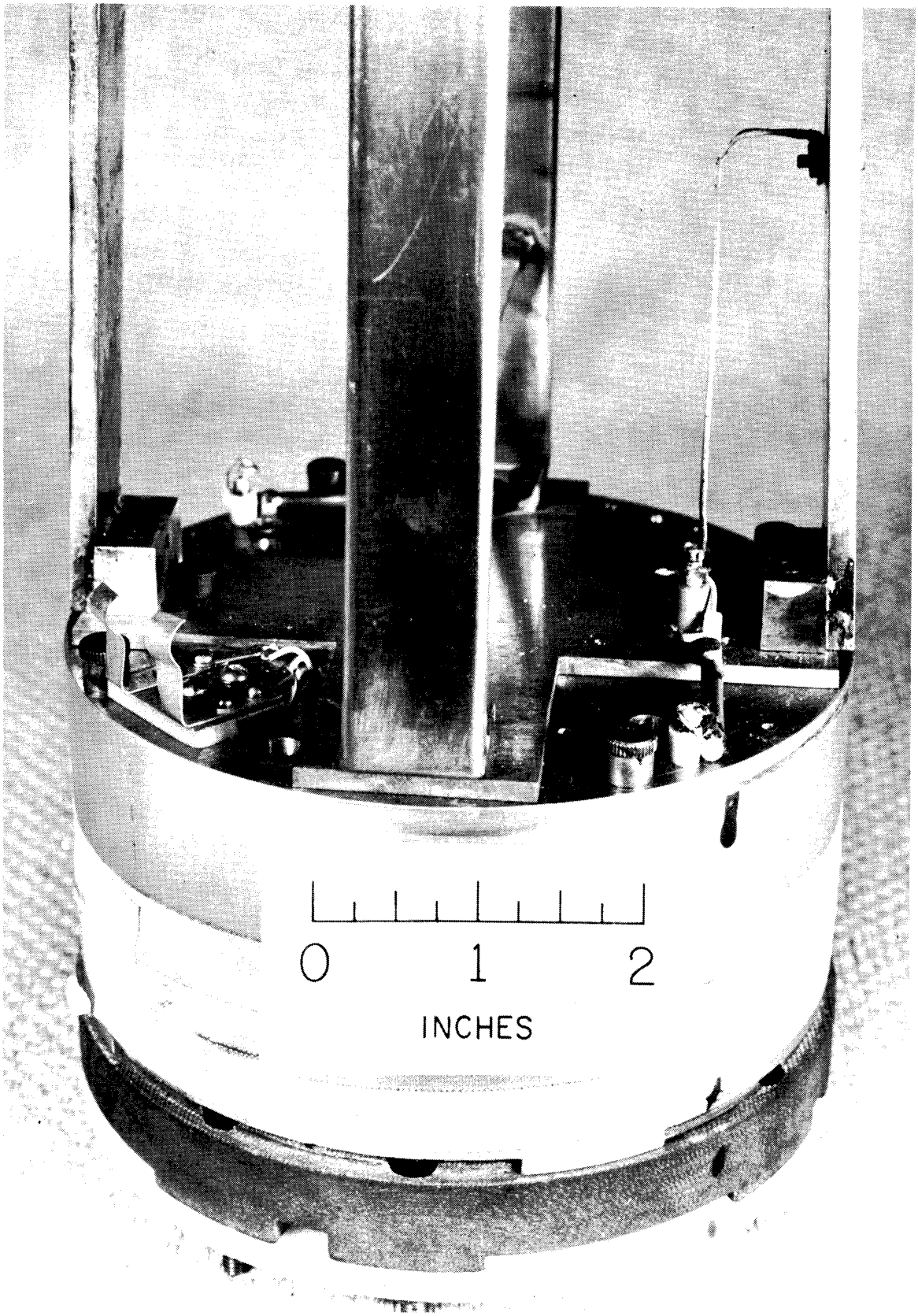

Fig. 32 Outside View of Beacon Assembly

5. THERMAL CONSIDERATIONS

5.1. THERMAL DESIGN OF BEACON PACKAGE

The two major problems in the thermal design of the beacon were (a) to produce an environment having temperature limits within which the mercury batteries, transistors, and other components can operate dependably, and (b) to produce a closely controlled temperature environment for the crystal oscillator so that a high degree of frequency stability is achieved.

Satisfactory component operation requires that the temperature remain between 5 and 75°C. This environment is furnished by the large thermal capacity of the beacon top plate, shell, and antenna (items 13, 14, 15, and 16 in Fig. 28). In addition, heat flow from the hot, burned-out rocket bottle is minimized by the fiberglass ring (item 19) and teflon plate (item 20). Because teflon is transparent to a large portion of the infra-red spectrum, radiation shields (item 22) of one mil aluminum foil are added to stop radiant heat from entering the package from below.

To produce a closely controlled temperature environment for the crystal oscillator, the heat of fusion principle was used. If the liquid and solid phases of a pure material, such as water, are present in thermal equilibrium, the temperature remains at the melting point. If heat is added or withdrawn from the container, its temperature will depart only slightly from the melting point, and by an amount sufficient to establish the required gradient between the container and the melting or freezing interfaces of the two phases.

Since water gave an unsuitably low operating point, the material used was a eutectic alloy,* Cerrolow 117. The properties of this alloy are as follows:

Melting point	=	47°C (117°F)
Heat of fusion	=	3.33 calories per gram
Density	=	8.85 grams per cm^3
Specific heat	=	0.035 calorie per °C per gram

The alloy chamber (item 11, Fig. 28) is filled with approximately 300 grams of alloy, allowing a small air space for expansion on melting. Thus approximately 1000 calories of heat can be absorbed by the oscillator case without any ap-

*This alloy is available at $8.69 per pound from Cerro de Pasco Sales Corporation, 300 Park Avenue, New York 22, N. Y. It is the lowest melting eutectic alloy commercially available, and has the following composition in percentage by weight: 44.7 Bi, 22.6 Pb, 8.3 Sn, 5.3 Cd, 19.1 In.

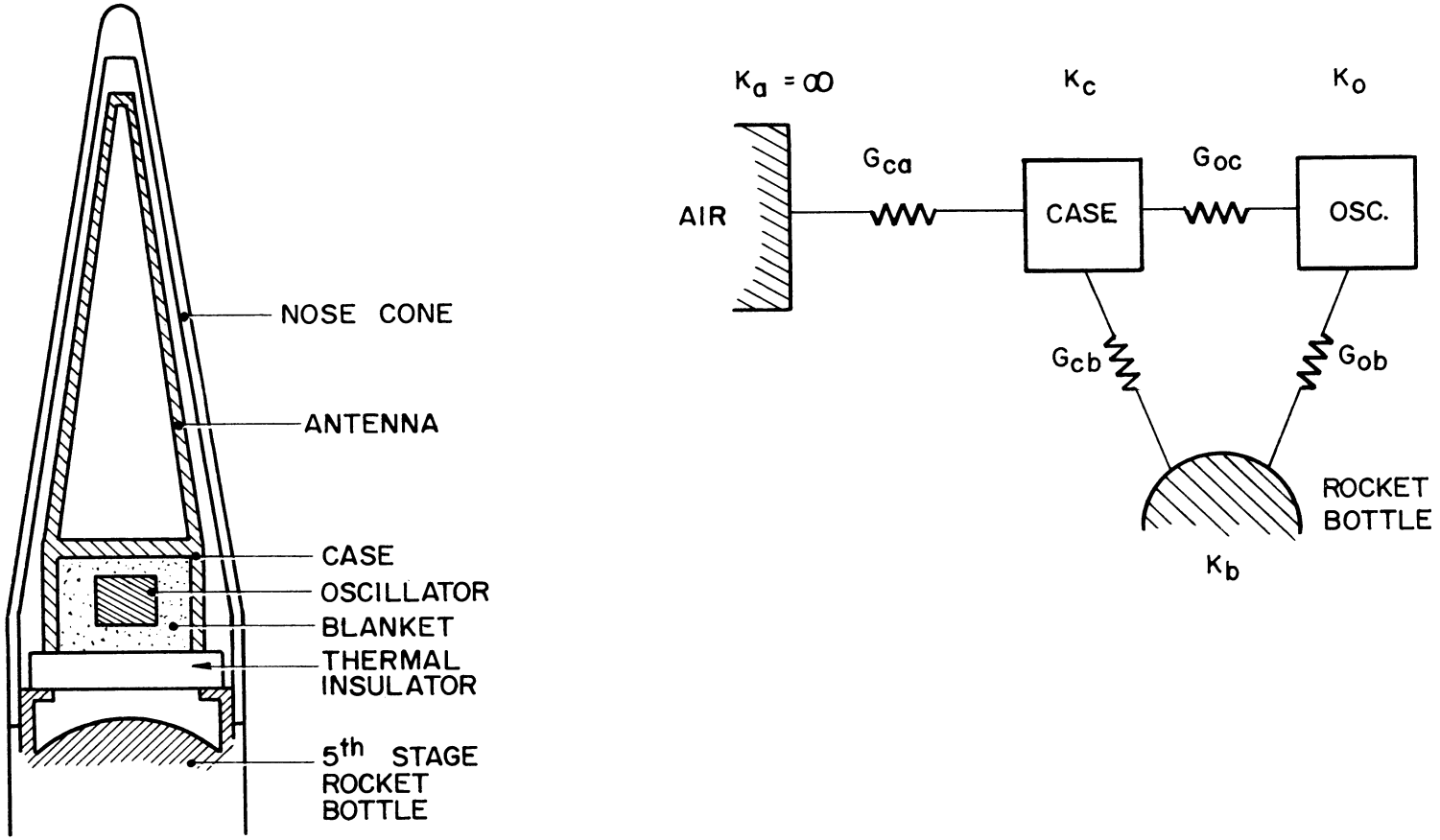

Fig. 33 Heat Exchange in Nose-Cone Assembly

preciable change in temperature. The crystal is located in the crystal well (item 10, Fig. 28) so that it is almost completely surrounded with alloy. The entire case is surrounded by a blanket of plastic foam (item 12) acting as an efficient thermal insulator, while being strong and rigid for mechanical support.

With this construction, and the heat exchange rates anticipated during flight, the crystal temperature is maintained within approximately ± 0.1°C of the melting point.

5.2. HEAT EXCHANGE AND THERMAL CONSTANTS

Heat exchange in the nose-cone assembly may be understood with reference to Fig. 33. Various items to be considered are diagrammed on the left while the important thermal masses and conductances are symbolized on the right. Subscripts a, b, c, and o refer respectively to the ambient air, the empty rocket bottle, case and antenna assembly of the beacon, and the oscillator unit.

For a systematic treatment, the following symbols are used:

Symbol	Quantity	Units
K	Thermal capacity	small calories/°C
$\dot{H}$	Heat flow	calories/min
θ	Temperature	°C
$\dot{\theta}$	Time derivative of temperature	°C/min
G_{ij}	Thermal conductance between i and j	calories/min per °C temperature difference between i and j
W_x	External electrical* heat input	watts

The basic equation for heat flowing into a body, i, is as follows:

$$\dot{H}_i = K_i\dot{\theta}_i = \sum_j G_{ij} (\theta_j - \theta_i) + 14.3\, W_x^* \qquad (6)$$

*Electrical heat input is given by $60\, W_x/J = 14.3\, W_x$ calories per min, where $J = 4.186$ joules per calorie.

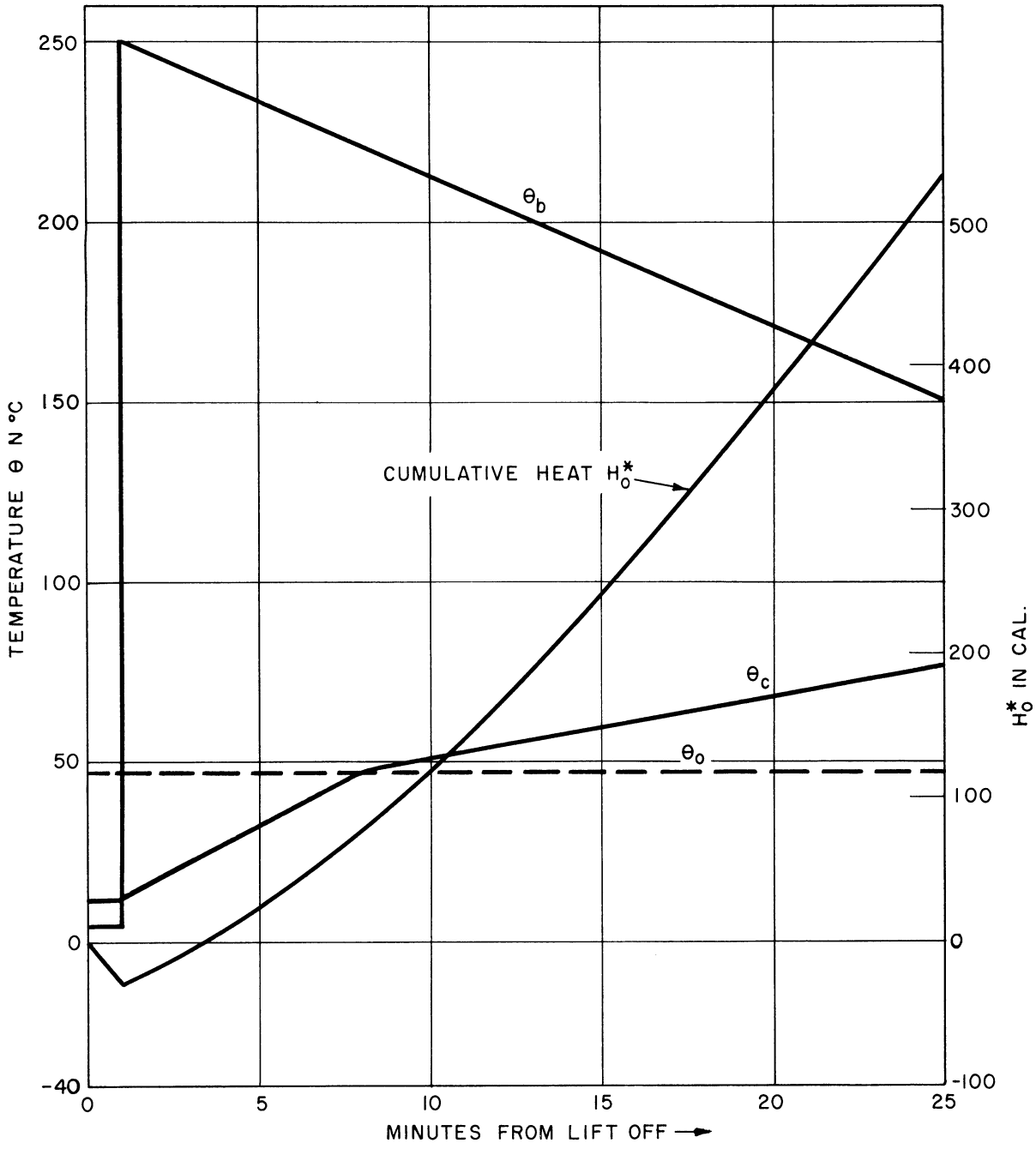

Fig. 34 Cumulative Oscillator Heat During Flight

Using experimental data taken both in the laboratory and on the launcher, and a suitable form of Eq. 6, the following values for the thermal constants were found:

G_{ob} = 0.131 calorie/min-°C

G_{oc} = 0.575 calorie/min-°C

G_{cb} = 0.82 calorie/min-°C

G_{ca} = 8.7 ± 1.0 calories/min-°C

} (Note 1)

K_o = 32.3 calories/°C (Note 2)

K_c = 250 calories/°C (Note 3)

K_a = ∞

K_b = 550 calories/°C (estimated)

Note 1. Values of conductances are for sea level. For vacuum flight, these values will be somewhat smaller.

Note 2. This value holds both above and below 47°C. However at 47°C, K_o is essentially infinite so long as the alloy is present in both solid and liquid phases. In this case approximately 1000 calories of heat may be added to the oscillator case with essentially no temperature change as previously explained.

Note 3. This checks closely with the computed value for the case and 1760 gram brass antenna. Thermal capacity of the case without the antenna assembly is 94 calories/°C.

5.3. HEAT EXCHANGE DURING FLIGHT

Probably the most important thermal aspect of the flight is oscillator temperature control. This section will therefore be concerned with heat exchange between the oscillator and its immediate environment.

At the time of take-off it will be assumed that the oscillator is at its operating temperature, and that sufficient of the alloy is melted to take care of any heat loss in the early part of the flight. It will be further assumed that the oscillator remains at 47°C for the entire flight.

By making the straight-line assumptions shown in Fig. 34 for probable beacon case and rocket bottle temperatures, a simplified thermal analysis may be made. The procedure is as follows.

TABLE I

PREFLIGHT PREPARATION OF BEACON TRANSMITTER PACKAGE

Step No.	Time "T" minus	Operation	Comments
1	---	Full power applied to case and oscillator heaters and transmitter for 15 seconds.	Safety and circuit check.
2	---	Residual case heat applied to maintain case temp. at 10 to 12°C.	Beacon batteries not dependable below 5°C.
3	2 hr	Case temp. raised to 35°C.	To store reserve heat.
4	---	All heaters off during arming of rocket. After arming completed, case temp. noted and residual case heat applied as necessary to maintain case temp. at 10 to 12°C.	Safety measure.
5	40 min	8 watts osc. heat applied. Osc. temp. noted until alloy begins to melt at 47°C. Heat on for further 15 seconds then removed.	Checks indicated melting temp. on control panel.
6	30 min	Osc. temp. noted; when it drops to 45°C, osc. heat finely adjusted to maintain this temp. Power noted. (1.7 watts for Nov. 10)	Temp. now close enough for frequency check.
7	8 min	Full osc. heat (17.5 watts) applied until θ_o = 47°C (alloy begins melting) and for an additional 100 seconds.	Net heat added for melting alloy = 370 calories.
8	6 min	After step 7, osc. heat dropped to 1.8 watts and held at this level.	Sufficient to furnish osc. heat loss at 47°.
9	3-1/2 min	All circuits disconnected from nose-cone assembly.	Osc. begins losing heat at 26 cal/min.
10	3 min	Pull nose-cone umbilicus.	
11	0	First stage fires.	Caloric reserve heat now reduced to 280 cal.

Heat flow into the oscillator is given by Eq. 6, i.e.,

$$\dot{H}_o = G_{oc} (\theta_c - \theta_o) + G_{ob} (\theta_b - \theta_o) \text{ calories per minute} \quad (7)$$

$$= 0.575 (\theta_c - 47) + 0.131 (\theta_b - 47) \text{ calories per minute} \quad (7a)$$

The cumulative oscillator heat H_o^* from take-off to +t minutes is obtained by integration:

$$H_o^*(t) = \int_o^t \dot{H}_o \, dt \quad (8)$$

Figure 34 also shows a plot of cumulative heat H_o^* found from Eqs. 7 and 8. It is seen that during the first minute of flight, 26 calories of heat are extracted from the oscillator. Thereafter, although some heat is lost to the case (for the first 8 minutes), more heat is acquired from the hot rocket, giving a net gain in heat for the remainder of the flight. At the end of 25 minutes (approximate time of splash), 530 calories of total heat have accumulated. Since this is well within the caloric capacity of the melting alloy, i.e., 1000 calories, the temperature of the oscillator remains constant at 47°C throughout the flight.

5.4. PREFLIGHT THERMAL PREPARATION

The paramount feature of preflight thermal preparation is the insurance that at take-off, sufficient alloy in the oscillator is melted to furnish heat losses for the first minute of flight, while leaving a sufficient reserve of solid material for the remainder.

Since the umbilicus is removed at T-3 minutes, and a safety margin of 10 minutes is desirable in the event of a hold in countdown after removing the umbilicus, sufficient alloy was melted to sustain the oscillator temperature at 47°C for about 14 minutes. Details of the thermal preparation are itemized in Table I. The table indicates a thermal reserve of 280 calories at firing time, which allows for a possible hold in countdown, a reserve for the first minute of flight, and any possible errors in computation.

Referring to the previous section, the oscillator accumulates 530 calories from firing until splash. With the above preparation, we have 280 + 530 = 810 calories, which leaves a flight margin of 190 calories before the 1000 calories of fusion heat are consumed.

A second feature of preflight thermal control, which applies only during cold weather, is that the package temperature must be maintained high enough to insure dependable operation of the mercury batteries. This is noted also in Table I.

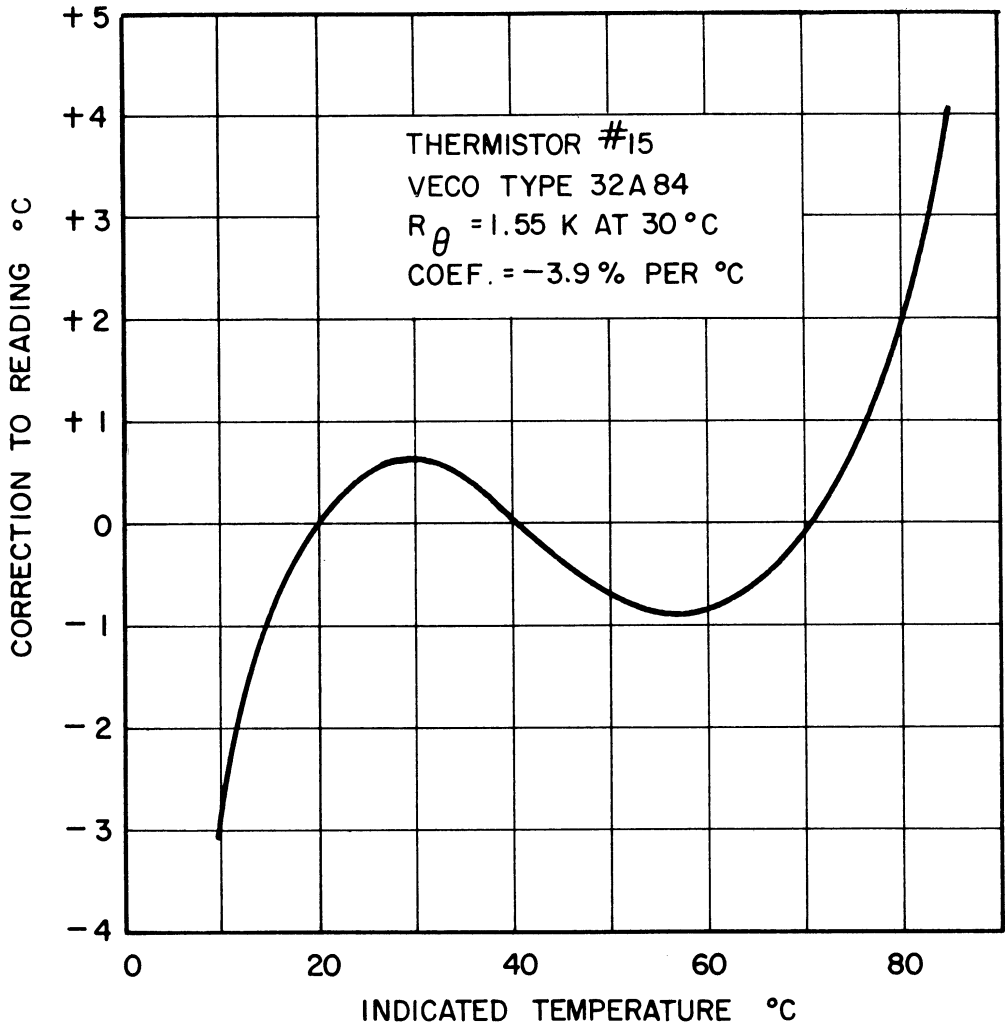

Fig. 35 Typical Correction Curve For Temperature Circuit

In the case of firing in sunny, hot weather, nose-cone temperature control would be required to keep the package temperature within reason. For conditions of little or no wind, and ambient temperatures below 35°C (95°F), a light-weight radiation shield of metal foil could be used. This could be pulled off with the umbilicus.

5.5. TEMPERATURE MEASUREMENT AND CONTROL

To indicate package (case) and oscillator temperatures of the beacon while on the launcher, temperature circuits were used in the ground station heater control panel. The circuit diagram of this is shown in Fig. 15. At the upper left, the package temperature circuit is seen to be a bridge circuit, the Type 32A84 VECO thermistor in the beacon package being connected to terminals 1 and 3 via the umbilicus and 1500-foot ground cable. The temperature is read directly with an accuracy of ± 1° between 15 and 75°C. For more accurate readings, a correction curve, Fig. 35, may be used.

Calibration of the circuit is performed by connecting two preset* resistance boxes to jacks J_{12} and J_{13}, and adjusting R_{11} and R_{12} until correct readings are obtained at 20 and 40°C in switch positions 3 and 4.

Two variacs on the heater control panel, Fig. 15, gave continuous control of heater power to the oscillator and package heaters. The indicating ammeters were calibrated in terms of the actual load currents flowing in the package, so that the wattage input to either heater was accurately known at all times.

*Preset to resistance values of the thermistor at 20 and 40°C when corrected for ground cable resistance.

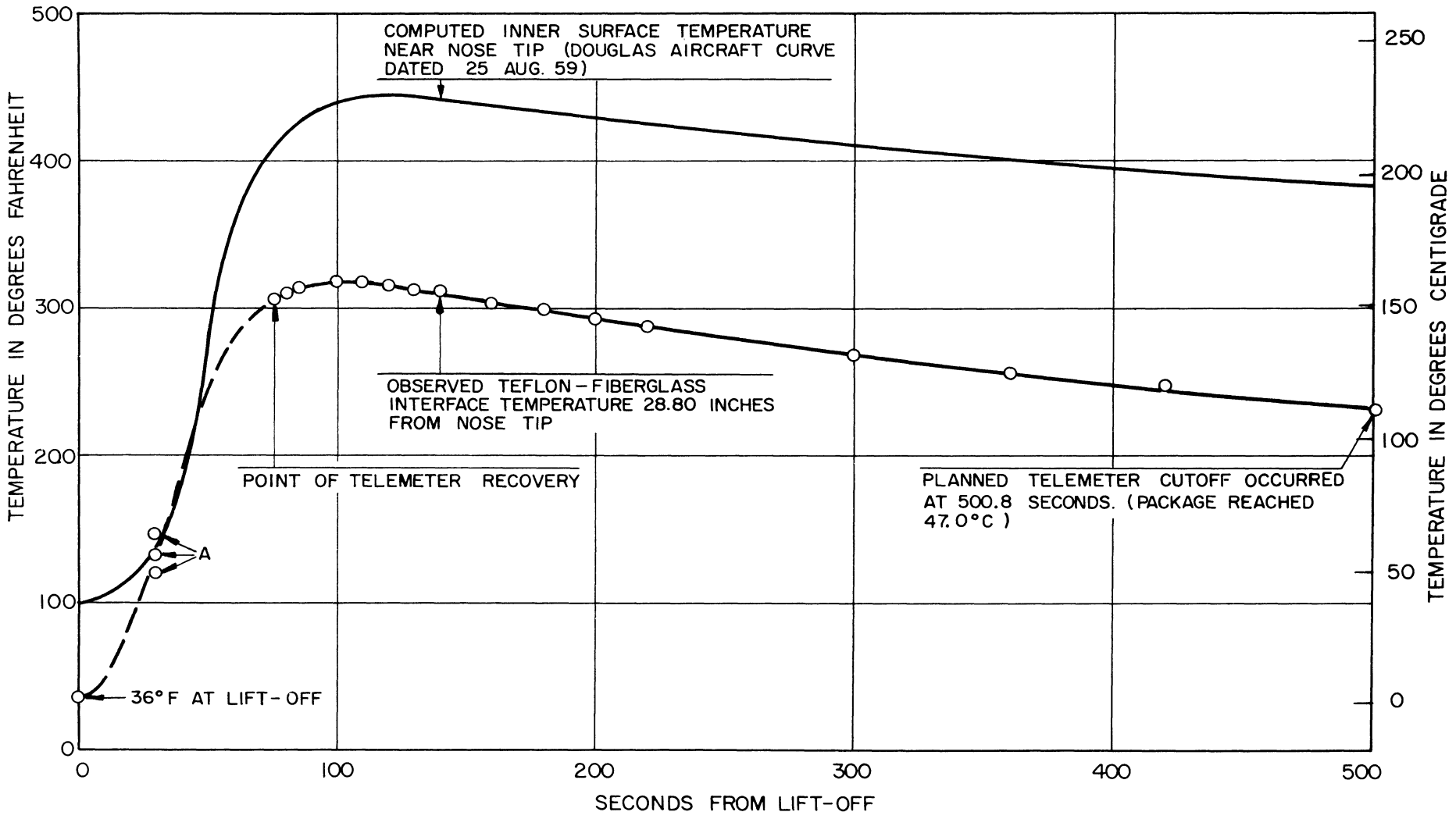

Fig. 36 Nose-Cone Temperature History

6. RESULTS OF THE NOVEMBER 10 FIRING

The firing of 10 November 1959 gave so much data that results on electron density profile are not available at this writing. However the telemeter record has been completely reduced, which gave the following results.

6.1. NOSE-CONE TEMPERATURE HISTORY

Figure 36 indicates the nose-cone temperature for the first 500 seconds of flight. The temperature was measured at the interface between the teflon coating and the fiberglass at a point 28.80 in. from the nose tip. The telemeter record indicates an open thermistor circuit for the first 76 seconds,* but at 77 seconds from lift-off, the circuit recovered and valid data were received. The temperature reached a maximum of 158°C (316°F) at about 100 seconds from lift-off.

6.2. BEACON-CASE TEMPERATURE HISTORY

Although only two points on the curve were obtained, a rough estimate of the temperature may be made as shown in Fig. 37. The point at 500 seconds was obtained by the planned telemeter cutoff which occurred when the beacon case reached 47°C (see Section 4.6).

6.3. SIGNAL DROOP AT 37 MC

Starting at about 37 seconds and ending at about 47 seconds, a droop of about 6 decibels was noted in the signal level as received by the Aberdeen and Wallops ground stations. During this period the inside pressure of the nose cone is changing from about 0.4 mm Hg to about 0.004 mm. This is a pressure range in which electric breakdown at rf is likely to occur if the voltage is sufficiently high. The rf voltage at the upper gap of the 37 Mc antenna with an input of 0.1 watt is 52.5 volts, and this is adequate to initiate a glow discharge. The signal droop is therefore attributed to rf breakdown of the air within the nose cone.

---

*Consecutive pulses, received at about 32 seconds gave 3 points (A in Fig. 36), which appear to be reasonably valid, indicating a temporary recovery at this time.

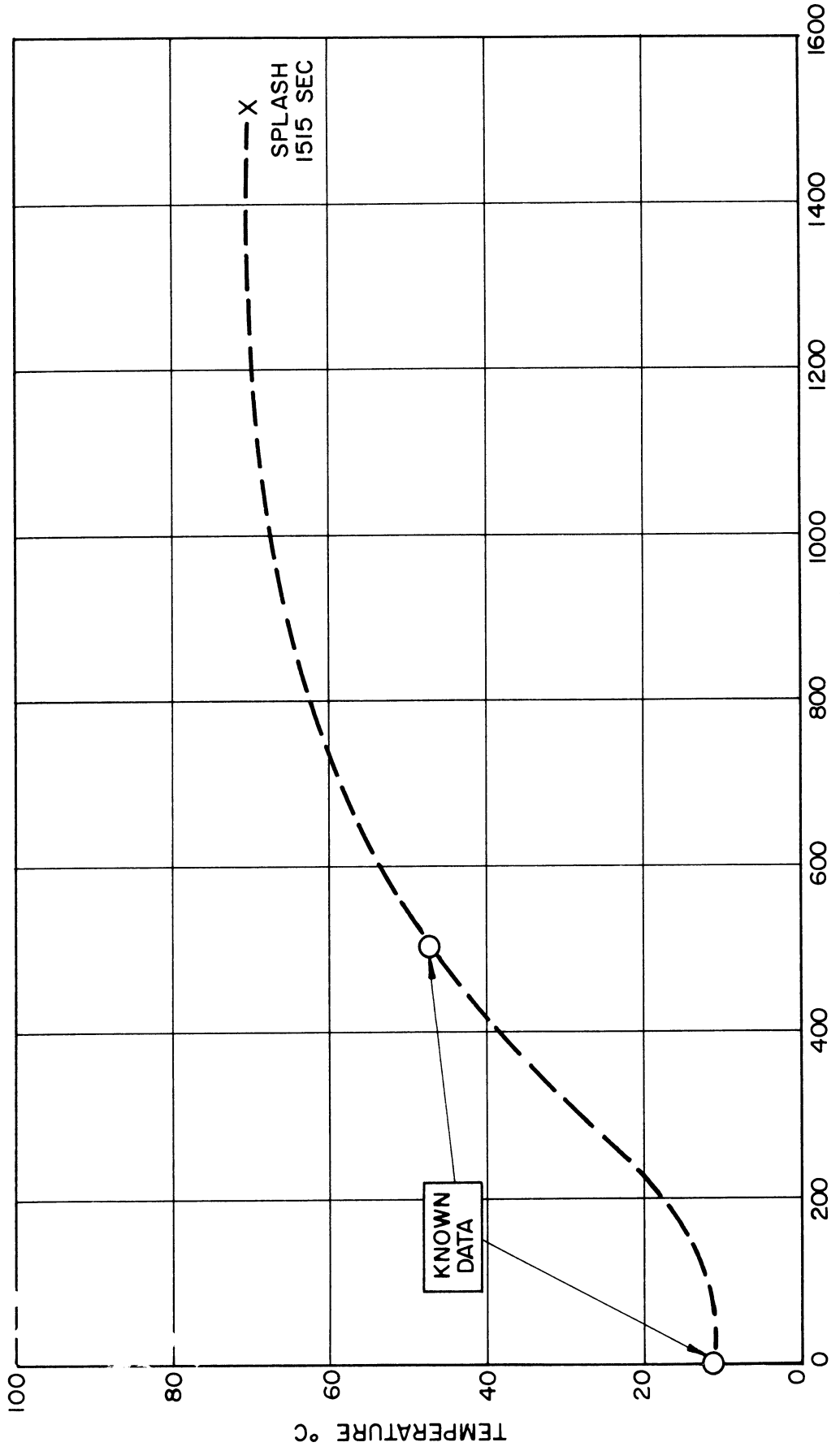

Fig. 37 Estimated Beacon Case Temperature History

7. CONCLUSIONS

The beacon package described above is considered a highly satisfactory design for high thrust rocket experiments. Although the design is quite conservative, both mechanically and electrically, no great reductions in weight, except for the antenna, could be made without sacrificing some aspect of performance or dependability.

Germanium transistors performed satisfactorily over the temperature range 0 to 80°C. For extended temperature ranges and more power (up to 1 watt at 37 Mc), silicon transistors could be used. However no suitable silicon transistors were available for the 148 Mc amplifier at the time of its design.

A high degree of frequency stability is obtainable in the adverse rocket environment by the use of a properly cut crystal, and the heat-of-fusion method of temperature control. In the November 10 flight, the crystal temperature was maintained within ± 0.1°C, giving a frequency stability better than one part in 10^8.

8. ACKNOWLEDGMENT

The success of this project was in no small measure due to the cooperation and assistance received from various members of the staff of the Ballistic Research Laboratories, The University of Michigan, and the Wallops Island Station of the National Aeronautics and Space Administration. In particular we wish to thank Messrs. W. W. Berning, V. W. Richard, and C. L. Wilson of the Ballistic Research Laboratories, and Messrs. N. W. Spencer, W. H. Hansen, and F. F. Fischbach of The University of Michigan.

9. PERSONNEL

Nelson W. Spencer	Project Director
Lyman W. Orr	Task Engineer
Pieter G. Cath	Research Associate
Bruce R. Darnall	Technician
Ancil S. Zeitak	Technician

DISTRIBUTION LIST

Ballistic Research Laboratory Aberdeen Proving Ground, Maryland Attn: Mr. Warren Berning	25
Detroit Ordnance District 574 East Woodbridge Detroit 31, Michigan Attn: Mr. Skeffington	2
The University of Michigan Ann Arbor, Michigan	
Nelson W. Spencer	2
Lyman W. Orr	2
Pieter G. Cath	2
Electronic Defense Group file	2
Engineering Library	1
Research Institute file	1